Journal of Medical Engineering & Technology, 2012; 36(6): 283–302

ISSN 0309-1902 print/ISSN 1464-522X online
DOI: 10.3109/03091902.2012.684830

informa
healthcare

REVIEW

Analysis of phonocardiogram signals using wavelet transform

F. Meziani, S. M. Debbal*, and A. Atbi

Genie Biomedical Laboratory (GBM), Faculty of Technology, University A. B. Belkaid-Tlemcen BP 119, Tlemcen, Algeria

Phonocardiograms (PCG) are recordings of the acoustic waves produced by the mechanical action of the heart. They generally consist of two kinds of acoustic vibrations: heart sounds and heart murmurs. Heart murmurs are often the first signs of pathological changes of the heart valves, and are usually found during auscultation in primary health care. Heart auscultation has been recognized for a long time as an important tool for the diagnosis of heart disease, although its accuracy is still insufficient to diagnose some heart diseases. It does not enable the analyst to obtain both qualitative and quantitative characteristics of the PCG signals. The efficiency of diagnosis can be improved considerably by using modern digital signal processing techniques. Therefore, these last can provide useful and valuable information on these signals. The aim of this study is to analyse PCG signals using wavelet transform. This analysis is based on an algorithm for the detection of heart sounds (the first and second sounds, S1 and S2) and heart murmurs using the PCG signal as the only source. The segmentation algorithm, which separates the components of the heart signal, is based on denoising by wavelet transform (DWT). This algorithm makes it possible to isolate individual sounds (S1 or S2) and murmurs. Thus, the analysis of various PCGs signals using wavelet transform can provide a wide range of statistical parameters related to the phonocardiogram signal.

Keywords: Phonocardiogram, Segmentation, Frequency, Duration, Wavelet transform Discrete parameters, Continuous parameters, Measurement, Statistics

1. Introduction

The heart is the principal organ that circulates blood in normal conditions. The exploration of its activity has become a very interesting field for cardiologists as well as researchers. There are two types of heart activity: electrical activity represented by the electrocardiogram signal (ECG) and a set of acoustic noises known as the phonocardiogram (PCG) signal [1]. PCGs are recordings of the acoustic waves produced by the mechanical action of the heart. They generally consist of two kinds of acoustic vibrations: heart sounds and heart murmurs [2].

The human heart generates four sounds during one cardiac cycle. These sounds, identified as S1, S2, S3 and S4 are not all audible [3].

The two hearts sounds: S3 and S4, with lower amplitude than S1 or S2 [3], appear occasionally in the cardiac cycle by the effect of disease or age.

The first heart sound, S1, corresponding to the beginning of ventricular systole, is due to the closure of atrioventricular valves. This sound is composed of two internal components: the mitral component (M1) associated with the closure of the mitral valve, and the tricuspid component (T1) associated with the closing of the tricuspid valve [5].

The second heart sound, S2, marking the end of ventricular systole and signifying the beginning of diastole, is made up of two main components: the aortic component (A2) corresponding to the closure of the aortic valve, and the pulmonary component (P2), corresponding to the closure of the pulmonary valve [6].

Before analysis, the PCG signal needs to be segmented into components (sounds or murmurs), and then the components analysed separately. Several techniques have been used to analyse the PCG signal components.

PCG signals have internal components of very close frequency bands. Fast Fourier transform (FFT) provides valuable frequency information about the heart sounds. However, FFT analysis remains of limited values if the stationary assumption of the signal is violated. Since heart sounds exhibit marked changes with time and frequency, they are therefore classified as non-stationary signals. To understand the exact feature of such signals, it is thus important to study their time–frequency characteristics.

Short-time Fourier transform (STFT) can provide the frequency and time duration of each heart sound [3]. However, it may not allow good resolution simultaneously in time and frequency [7].

Wavelet transform (WT) has demonstrated the ability to analyse the heart sound more accurately than other techniques

*Corresponding author. Email: adebbal@yahoo.fr

such as STFT or Wigner distribution [8]. This technique has been shown to have a very good time resolution for high-frequency components. In fact, the time resolution increases as the frequency increases and the frequency resolution increases as the frequency decreases [5,9].

In the next section, this technique will be described in detail.

2. Materials and methods

We propose a method based on discrete wavelet transform (DWT) in combination with continuous wavelet transform (CWT), which is used in the analysis of various PCG signals. Several statistical parameters are deduced from the application of wavelet transform that allow more understanding of cardiac activity and at the same provide a valuable aid to clinicians [10].

2.1. Wavelet transform

Wavelet transform allows multi-resolution analysis. It is based on the use of a special function called the mother transform. This function undergoes translation and contraction or dilatation operations to give a set of functions called wavelets. These functions are a constant shape but variable size. When the studied signal is analysed by wavelets, a set of coefficients are obtained. These coefficients represent the correlation between the wavelet and the studied signal. They are given by equation (1).

$$\psi_{a,b}(t)=\left(\frac{1}{\sqrt{a}}\right)*\frac{\psi(t-b)}{a} \qquad (1)$$
$$a\in R, b\rangle 0$$

where a represents the scale and b the translation coefficient. The wavelet transform (WT) applies a multi-resolution analysis on the signal studied. This analysis can be called the time-scale, and uses a wide range of scales to analyse the signal. When the a and b factors are continuous, the wavelet transform is a continuous wavelet transform (CWT) (equation 2). CWT is used when no reconstruction of the original signal from the obtained coefficients is needed. Conversely, when the original signal needs to be reconstructed, discretization of the a and b factors must be carried out. The obtained wavelet is named discrete wavelet transform (DWT). Discretization can be done by equation (3).

$$w_x(a,b)=\left(\frac{1}{\sqrt{a}}\right)\int_{-\infty}^{+\infty}x(t)\psi^*(t-b)/a\,dt \qquad (2)$$

$$a=2^j, b=k2^j (j,k)\in Z \qquad (3)$$

One of the efficient ways to construct the DWT is to iterate a two-channel perfect reconstruction filter bank over the low pass scaling function branch. This approach is also called the Mallat algorithm [11]. DWT theory requires two sets of related functions called scaling function and wavelet function, which are given by:

$$\varphi j(t)=\sum_{n=0}^{N-1}h[n]\sqrt{2}\varphi j(2t-n) \qquad (4)$$

$$\psi(t)=\sum_{n=0}^{N-1}g[n]\sqrt{2}\varphi(2t-n) \qquad (5)$$

where function $\varphi(t)$ is the scaling function and $\psi(t)$ is the wavelet function, $h[n]$ is an impulse response of a low pass filter and $g[n]$ is an impulse response of a high-pass filter [12].

The scaling function and wavelet functions can be implemented using pair of simple low-pass and high-pass filters. If the filters are interpreted with their impulse responses as $\{h(n), n\in N\}$ for a low-pass filter and $\{g(n), n\in N\}$ for a high-pass filter, then the decomposition of a signal using

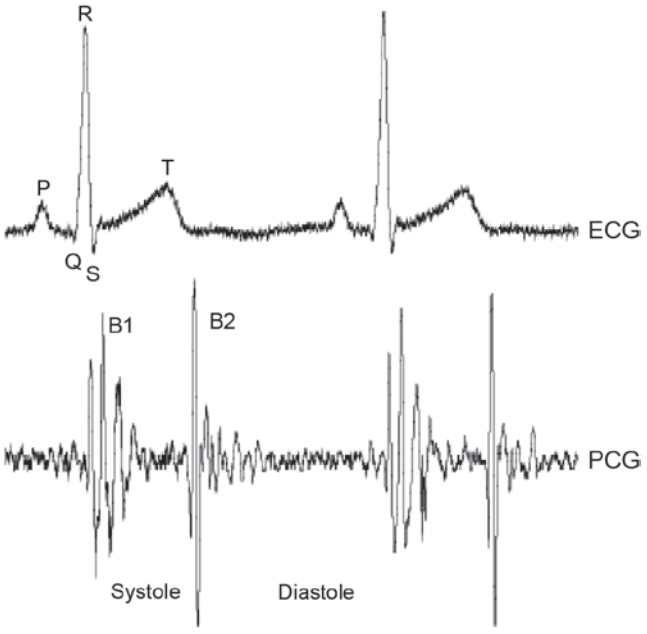

Figure 1. Electrocardiogram and phonocardiogram signals of a healthy subject.

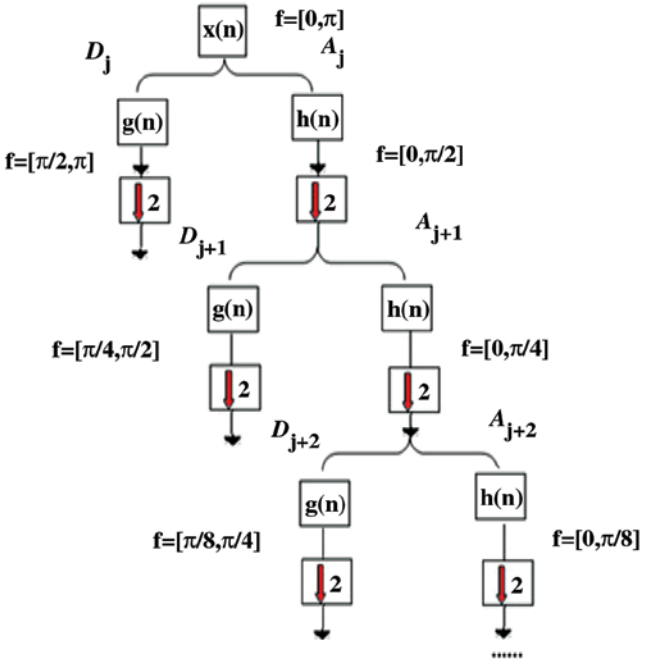

Figure 2. Signal decomposition using DWT.

DWT will be as shown in Figure 2. This decomposition is also termed dyadic decomposition. The first stage divides the frequency spectrum into two equal parts (low pass and high pass). The second stage then divides the low-pass band into another low-pass and high-pass band .The second stage divides the lower half into quarters, and so on [12].

2.2. Denoising by wavelets

Our aim with this denoising is to extract the heart sounds (S1 and S2) of murmurs that are considered in this stage as noise. Denoising, or noise reduction, is a permanent topic for engineers and applied scientists. The model considered for denoising is classic: the measured signal X is an additive mixture of an information signal S and a measurement noise R [12]:

$$X(t) = S(t) + R(t) \tag{6}$$

Denoising by thresholding the wavelet coefficient, as defined in [13], is used to extract a coherent structure of the measured signal. The hypothesis considers that the noise as a not coherent with a waveform database predefined:uncorrelated with these waveforms. The coefficients of the decomposition of noise on the base are low, so they can be easily removed.

The most commonly used algorithm is the decomposition of a discrete wavelet orthonormal basis of Mallat [6]: simple decomposition and reconstruction exact. After decomposition of the signal on this basis, the segments less correlated with the base of the coefficients are low, and they are attributed to noise. A suitable threshold can separate the noise (incoherent part) from the signal (coherent part). The denoised signal is generated through inverse reconstruction (IDWT). This procedure is shown in Figure 3. Vos [14] and Messer *et al.* [15] used this approach in phonocardiogram signal denoising.

In the literature, there are two types of thresholding: hard thresholding and soft thresholding [16]. The first proposes the collation of all values below a threshold T, with the higher values unchanged ($w_{j,k}$: coefficients of the decomposition of the signal x).

$$w_{j.k} = \begin{Bmatrix} w_{j.k} \; if \left|w_{j.k}\right| > T \\ 0 \;\; if \left|w_{j.k}\right| \le T \end{Bmatrix} \tag{7}$$

The second method operates in addition to the cancellation, with a subtraction of the threshold values remaining above the threshold, to reduce the number of discontinuities in the denoised signal.

$$w_{j,k} = \begin{cases} sign(w_{j,k})(\left|w_{j,k}\right| - T) & if \left|w_{j,k}\right| > T \\ 0 \; if \left|w_{j,k}\right| \le T \end{cases} \tag{8}$$

The threshold T can be calculated in different ways. The method chosen in our algorithm was developed by Donoho and Johnstone [17], known as universal thresholding.

Before applying wavelet denoising, we must consider some parameters, such as the type of wavelet used, the decomposition level selected and the type of thresholding.

2.2.1. *The choice of the mother wavelet*

Analysis of PCG signals using wavelet transform has shown that it is important to determine the appropriate wavelet. In this work, we use two types of wavelet: Daubechies and Morlet. The study carried out on different types of orthogonal and bio-orthogonal wavelet at different levels using standard deviation and error of rebuilding as a discrimination parameter has shown that the Daubechies wavelet of the seventh level (db7) can be used in PCG signal analysis. In fact its morphology and duration are highly correlated to the different sounds in the PCG [18].

The Morlet wavelet also has value due to its shape, which is very similar to heart sounds [19,20]. The Morlet wavelet in two aspects (real and complex) is shown in Figure 4.

The complex wavelet is more suitable than the real one for our study, as it provides a representation properly localized in time. However the real wavelet provides a representation with temporal interference [21–24].

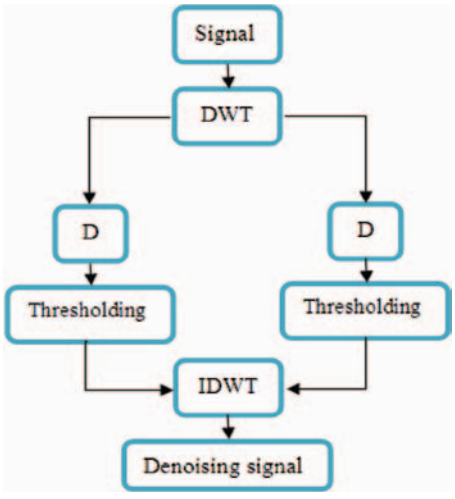

Figure 3. Diagram of wavelet denoising (thresholding).

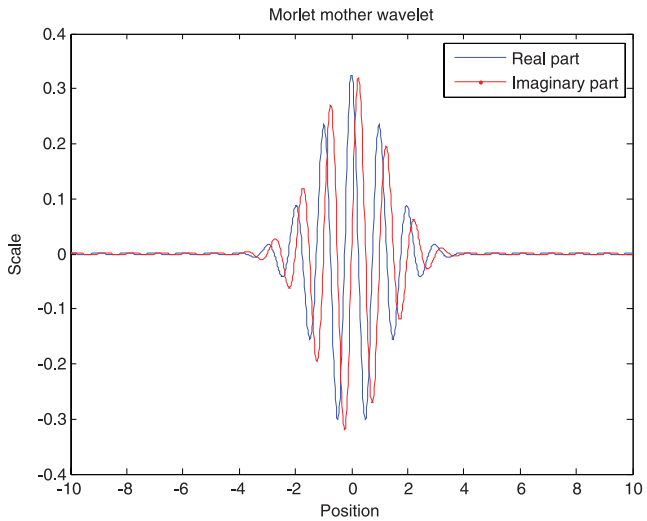

Figure 4. Morlet wavelet: part real and imaginary part.

2.2.2. The decomposition level selected and the type of thresholding

Messer *et al.* [15] found that the 10th level of decomposition is the best for denoising PCG signals sampled by 44.1 kHz, where they used the Daubechies wavelet of the seventh level (db7). Moreover, they proved that the universal soft thresholding gives satisfactory results.

The sampling frequency of the PCG signal has a great influence on the appropriate decomposition level for denoising. To show the influence of sampling frequency on the optimal decomposition level, Figures 5–7 show a PCG signal generated with two different sampling frequencies.

In the first case (Figure 6), the optimal denoising is successful at the fifth level; beyond this level the signal begins to distort. For the second case (Figure 7), ideal denoising appears at the seventh level; however, few traces remain of murmurs. Indeed the decrease in signal distortion relative to the increase in sampling rate can be explained as follows.

In first case, fs = 8 kHz, the signal converges rapidly to the deformation; however the limited number of samples makes a perfect denoising operation. With a sampling frequency of 44.1 kHz, the number of samples is sufficient and the resolution is still good; therefore, the reconstructed signals are slightly deformed. However, the high number of samples makes the process of denoising worse.

In our work, and in order to have good filtering, we chose 8 kHz as the sampling frequency for all PCG signals that will

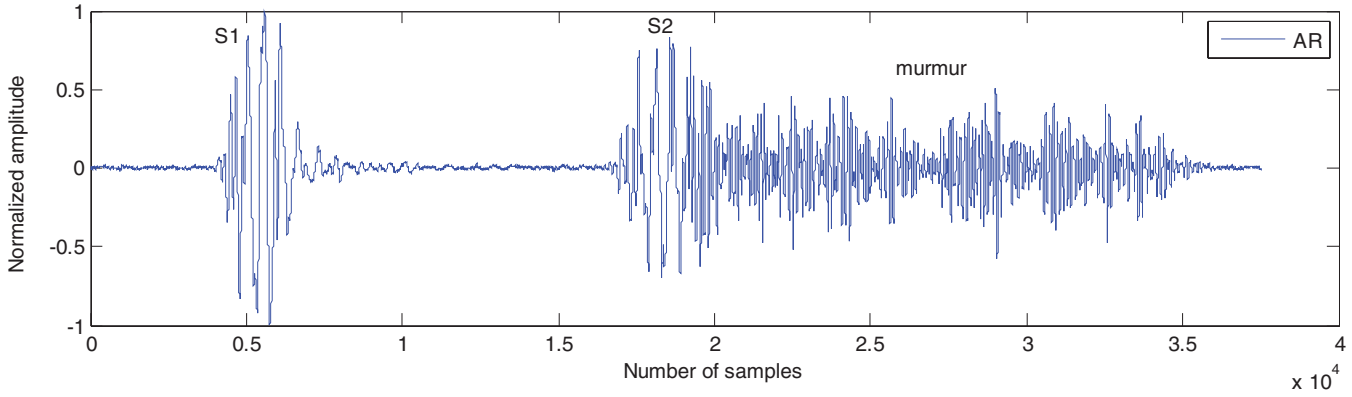

Figure 5. Phonocardiogram signal with a diastolic murmur (aortic regurgitation).

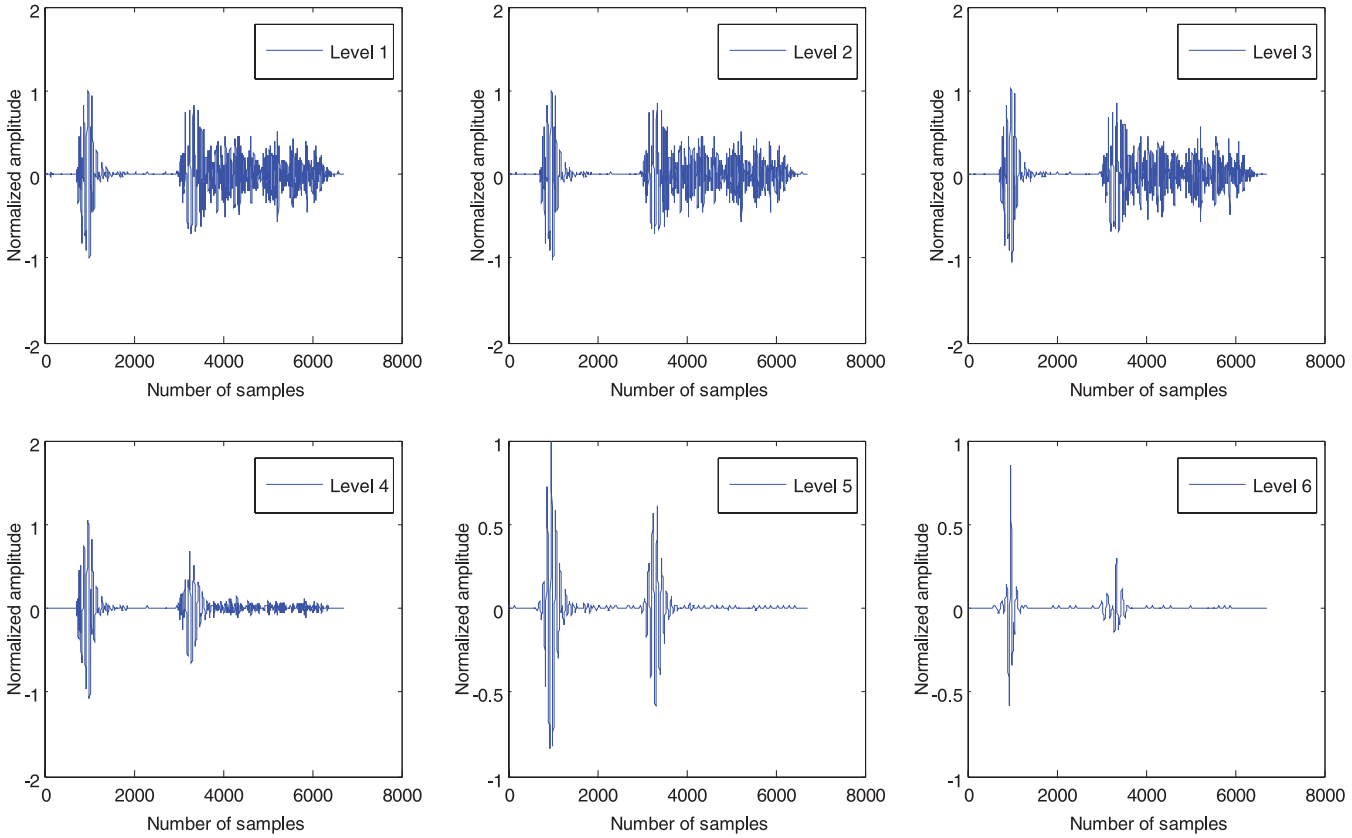

Figure 6. Wavelet denoising of the signal presented in figure 5 on different levels of decomposition. The sampling frequency is 8000 Hz.

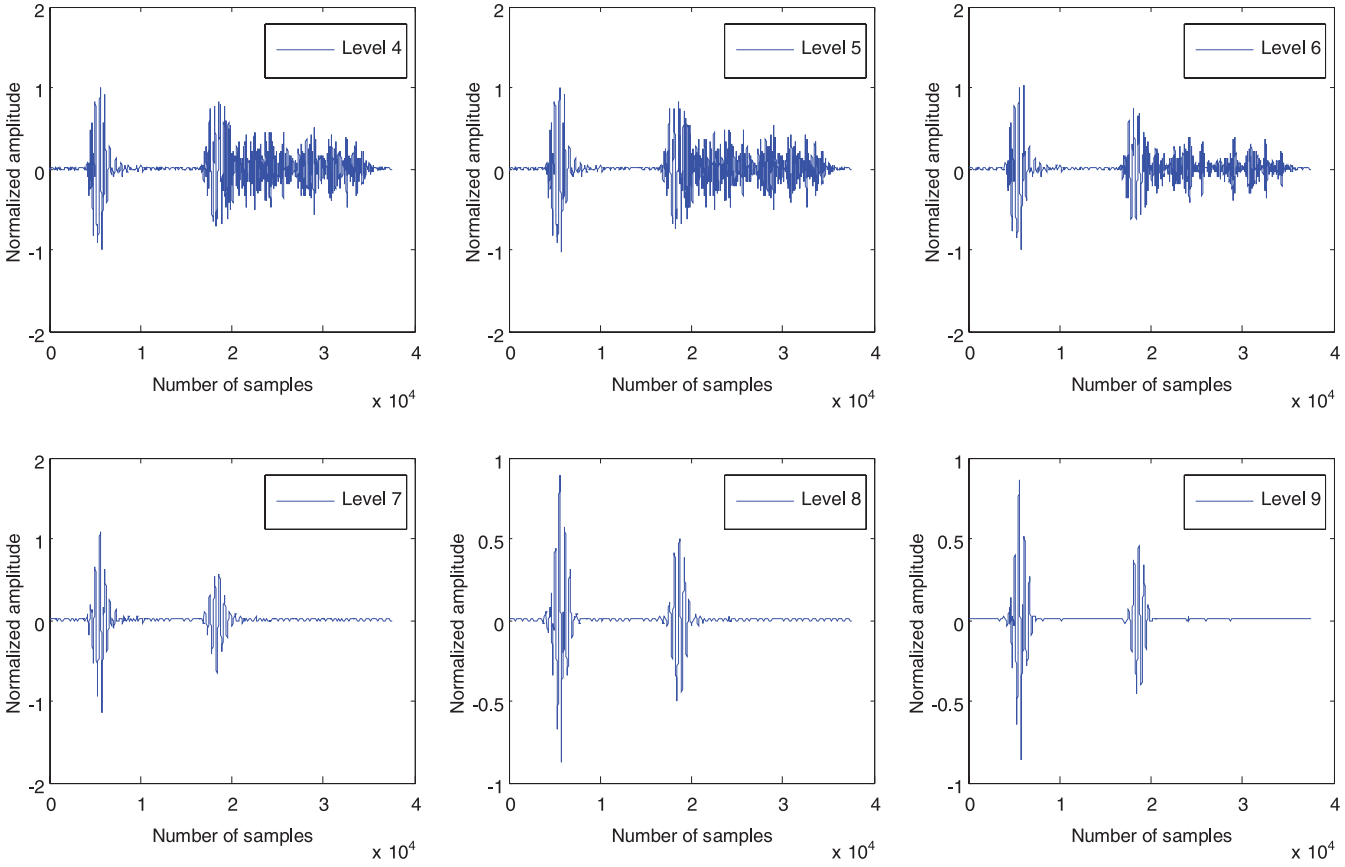

Figure 7. Wavelet denoising of the signal presented in figure 5 on different levels of decomposition. The sampling frequency is 44.1 kHz.

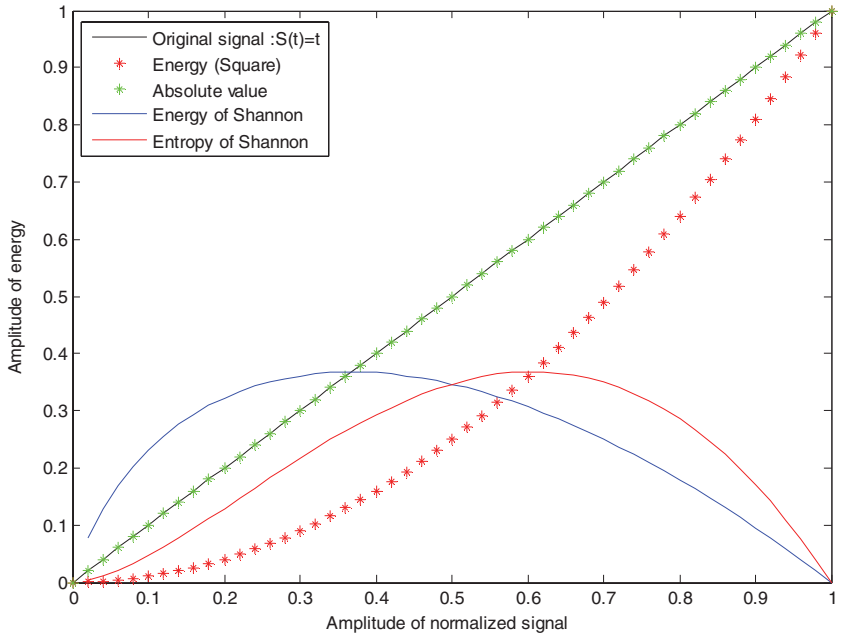

Figure 8. Temporal energy representation of the signal S(t).

be addressed. Changing the sampling frequency is performed by software sound processing (WAVEdit).

The proposed approach to separate the components of the PCG signal is also based on the detection of the temporal energy envelope of the PCG signal. The temporal lobes of the energy of the PCG signal are correlated with intracardiac events. Shannon energy can better represent the oscillations of small amplitude, not just large amplitude oscillations [19].

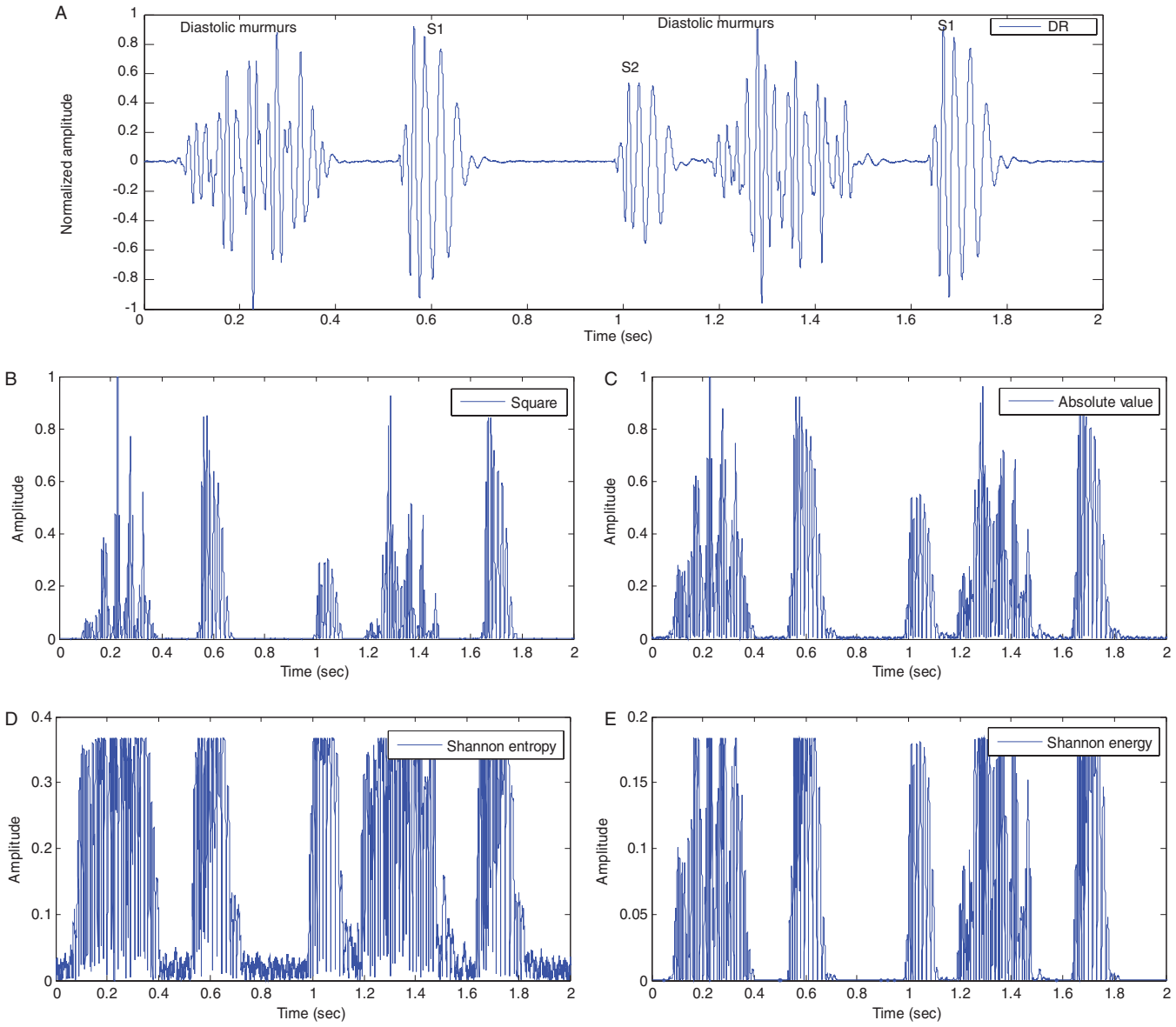

Figure 9. Energy representations of a pathological PCG DR (drum rumble) signal. (a) PCG signal; (b) squared PCG signal; (c) absolute value of the PCG signal; (d) Shannon entropy of the PCG signal; (e) Shannon energy of the PCG signal.

2.3. Study of energy

Some attempts to extract the PCG envelogram have been reported in the literature. One such approach works by creating the analytical signal of the input by using a Hilbert transform. However, there are other methods to extract the envelope as the calculation of the square of the signal or absolute value (equations (9–10)).

The square of the samples of a given signal (equation (9)) makes it possible to evaluate its energy in the temporal field. However, and as illustrated in Figure 8, samples of high amplitude are very heavily favoured over those of low amplitude. The amplitude of the energy calculated by the absolute value (equation (10)] of the samples of the signal also disadvantages samples of low amplitude.

Two other approaches that can be used are Shannon entropy and Shannon energy; see equations (11) and (12). These approaches give greater weight to the average intensities of the signal; therefore, the noise of low intensity and high intensity of disturbance will be mitigated. Similarly, the Shannon entropy (equation (11)) does not yield the true proportions of the signal, attenuating more samples of very low amplitude for the benefit of large-amplitude oscillations. The Shannon

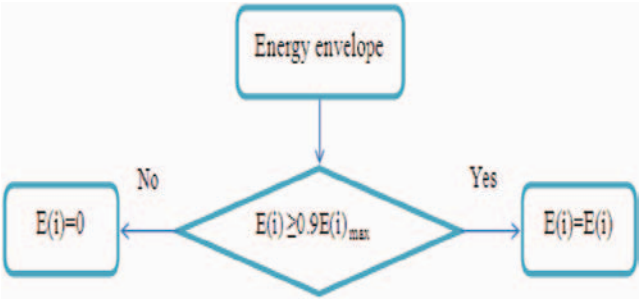

Figure 10. Algorithm to remove values below 90%.

energy (equation (12)) proves the median approach, making it possible to generate a representation that takes account of the physiological attenuation of heart sounds as well as artefacts of large amplitude while recording the PCG signal.

- Square of the energy:

$$E = S^2(t) \tag{9}$$

- Absolute value of the energy:

$$E = |S(t)| \tag{10}$$

- Shannon entropy:

$$E = -|S(t)|^{*}\log|S(t)| \tag{11}$$

- Shannon energy:

$$E = -S^2(t)^{*}\log S^2(t) \tag{12}$$

The PCG signal energy representations (Figure 9) highlight the interest of the Shannon energy. According to these figures, we can see that only the Shannon entropy and the Shannon

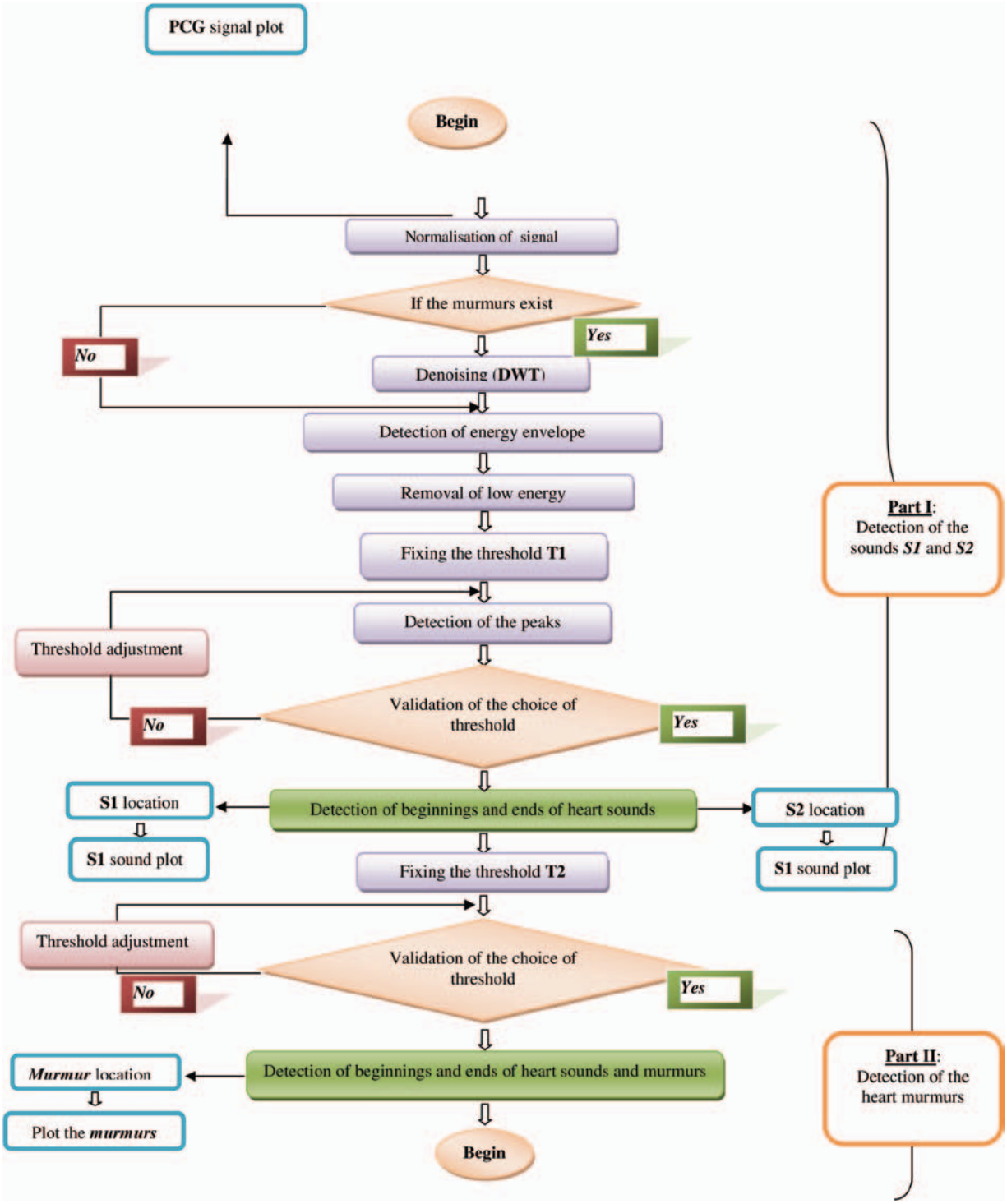

Figure 11. Algorithm of separation of heart sounds and heart murmurs.

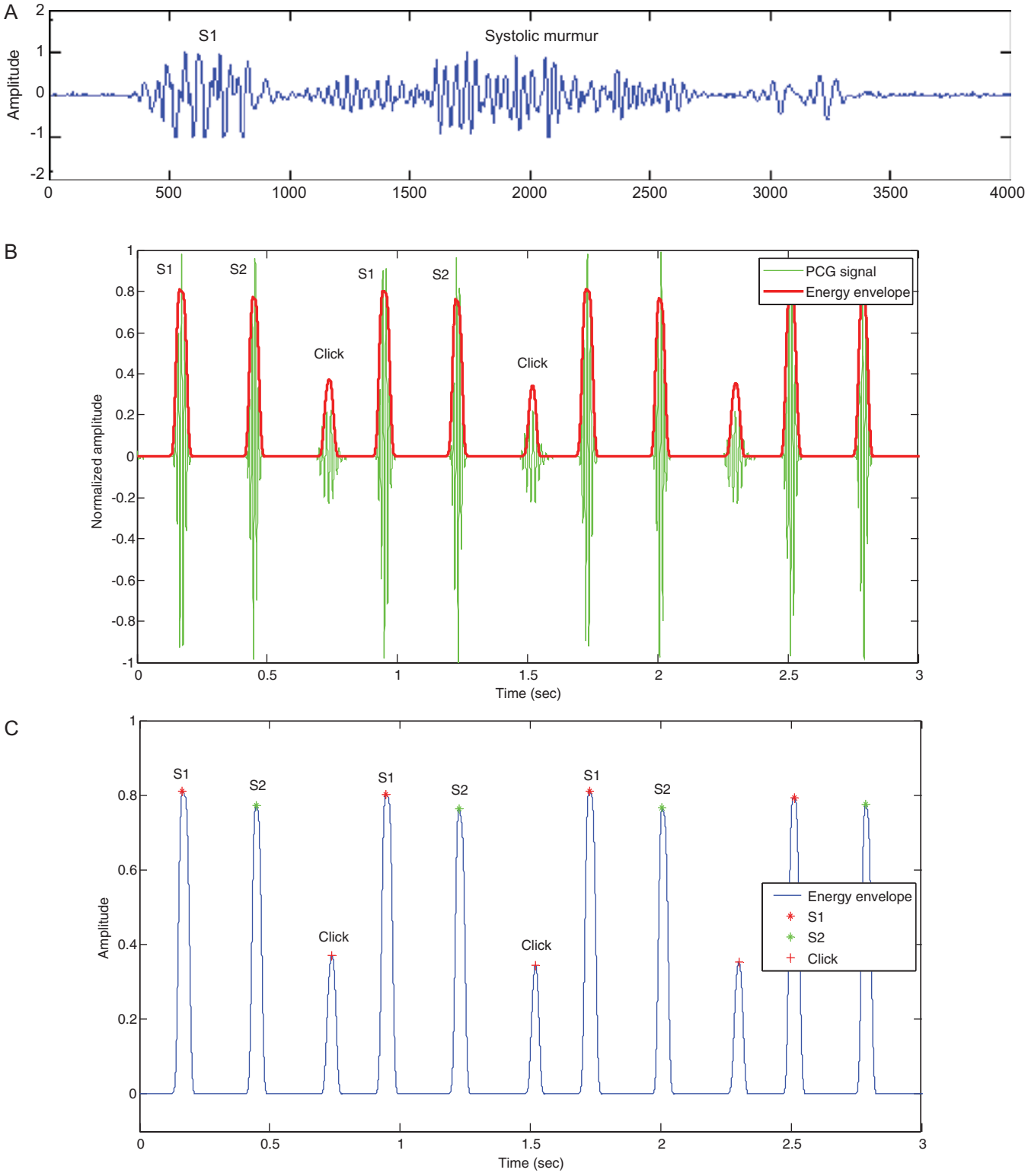

Figure 12. PCG signal of subject with aortic stenosis. (b) Detection of the envelope and identification of sound B1, B2 and murmurs; (c) the total energy of Shannon superimposed on the PCG signal.

energy can absorb the magnitude of oscillations of high intensity as well as those in low amplitudes. The shape of the curve of the Shannon energy promotes weak oscillations, which will give energy representations that take into account the unit of the heart sounds and heart murmurs. Indeed, as illustrated in Figure 9, we can see the value of the Shannon energy (Figure 9(e)) compared to the other methods used. The Shannon energy places more emphasis on oscillations of low amplitude while also representing those of high amplitude. Thus, the Shannon energy is used in PCG segmentation.

2.3.1. Detection of the envelope of the energy signal

The separation algorithm depends primarily on the detection of the Shannon energy envelope, which easily identifies the beginnings and ends of the cardiac sounds S1 and S2. This envelope is extracted by applying a low-pass filter, with a cut-off frequency f_0 of 20 Hz, chosen empirically. This filtering is reinforced by an algorithm to remove low energies below 90% from the maximum (Figure 10).

3. The proposed algorithm

Valvular heart diseases induce considerable changes in the morphology of the phonocardiogram signal. These changes can be seen as a change in duration, amplitude or the frequency content of sounds S1 and S2 or systolic and diastolic murmurs. These parameters must be calculated in a precise manner to allow a proper assessment of severity. Therefore, segmentation of the PCG signal appears important to facilitate this task.

The aim of this section is to develop an algorithm for heart sound and heart murmur location and separation, and to measure the various time and frequency parameters. The proposed PCG segmentation algorithm is shown in Figure 11.

Several algorithms based on energy envelope detection have been proposed [25–27]. These approaches are effective in cases where the power of sounds S1 and S2 is much higher than the murmurs, but they quickly find their limit when the power of murmurs is almost the same as or higher than the sound.

Therefore, applying denoising by wavelet transform (DWT) in our algorithm is very important to solve this problem. In fact, as the frequency content of murmurs is more important than those sounds, DWT can be separated easily by technique of the denoising by thresholding (wavelet denoising).

This algorithm (Figure 11) has six main parts:

(1) Pretreatment: Detection of the envelope of the Shannon energy; make the appropriate for the detection of sounds.
(2) Identification of S1 and S2.

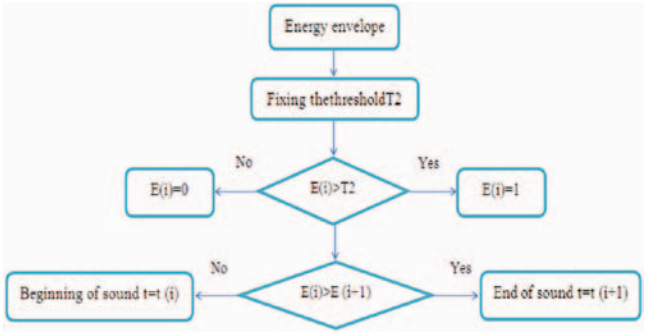

Figure 13. The algorithm for detecting minimum side of each sound.

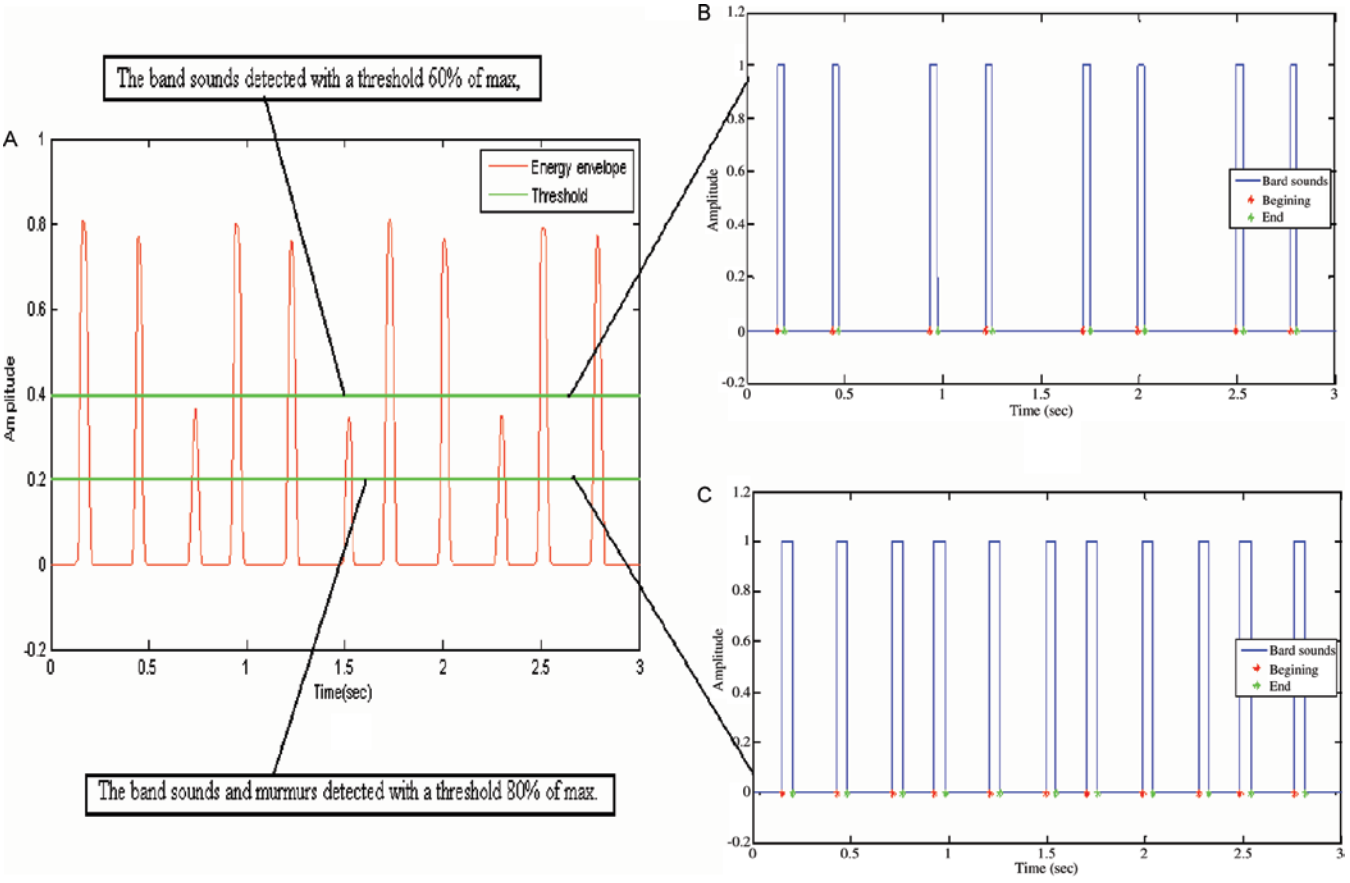

Figure 14. (a) The envelope of the PCG signal with a threshold at 60% and 80% of the maximum; (b) the band sounds detected with a threshold of 60% of the maximum; (c) the band sounds and murmurs detected with a threshold of 80% of the maximum.

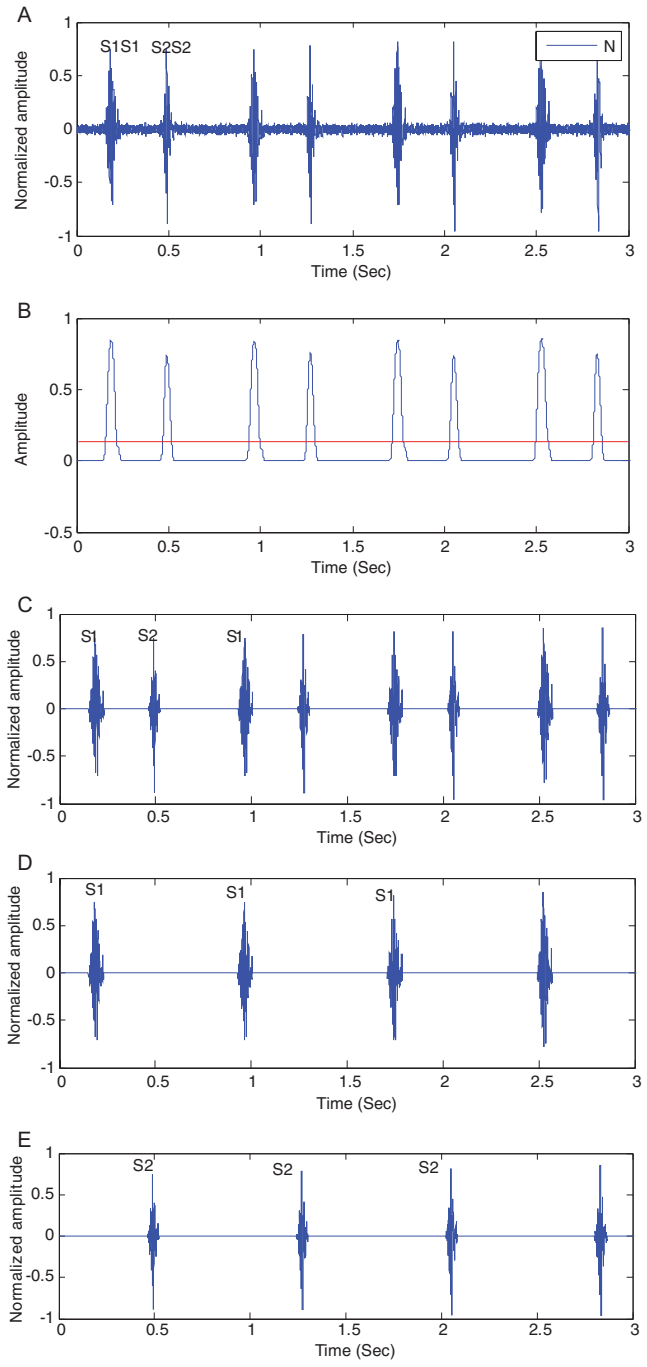

Figure 15. Insulation of heart sound: (a) PCG signal—N (normal); (b) energy envelope with a threshold of 90% of the maximum value; (c) heart sounds S1 and S2; (d) heart sound S1; (e) heart sound S2.

(3) Extraction of sounds.
(4) Identification of murmur.
(5) Extraction of murmurs.
(6) Treatment of sounds and murmur, such as measurement of the duration, the frequency range, in a graphic manner using the time–frequency representations by applying the Morlet wavelet CWT.

All these parameters will be considered to analyse the PCG signals.

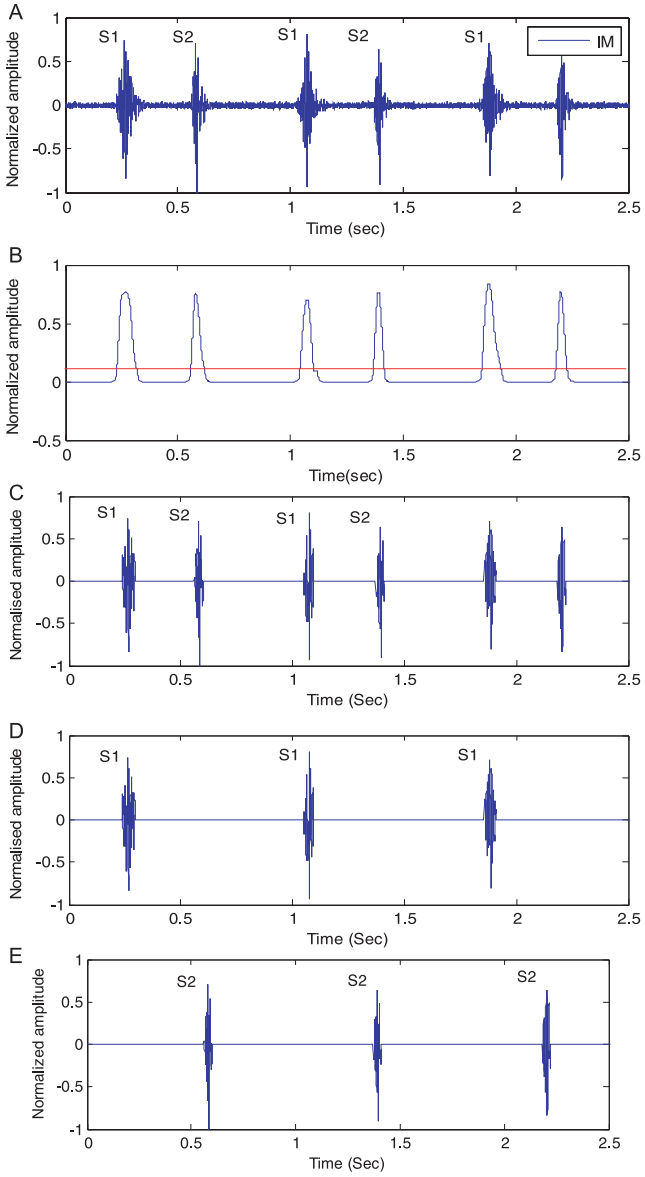

Figure 16. Insulation of heart sound: (a) PCG signal—IM (innocent murmur); (b) energy envelope with a threshold of 90% of the maximum value; (c) heart sounds S1 and S2; (d) heart sound S1; (e) heart sound S2.

Due to the complexity of the phonocardiogram signal, our algorithm (Figure 11) consists of a supervised manner: the user must adjust some parameters to achieve optimal segmentation (e.g. threshold and decomposition level).

After normalization of the PCG signal the user has the choice to perform discrete wavelet decomposition (DWT). This step is necessary if the murmurs present a high intensity (Figure 12). The frequency content of heart murmurs is more important than the heart sounds (S1 and S2), for that, the DWT can be used as a filtering means relatively simple and very effective to remove high frequency components. The envelope is detected by applying a low-pass finite impulse response (FIR) filter.

3.1. Detection of S1 and S2 heart sounds

The sampling rate used is 8000 samples/s. The optimal denoising appeared in the fifth level of decomposition; the reconstructed signal in this level is used in the detection

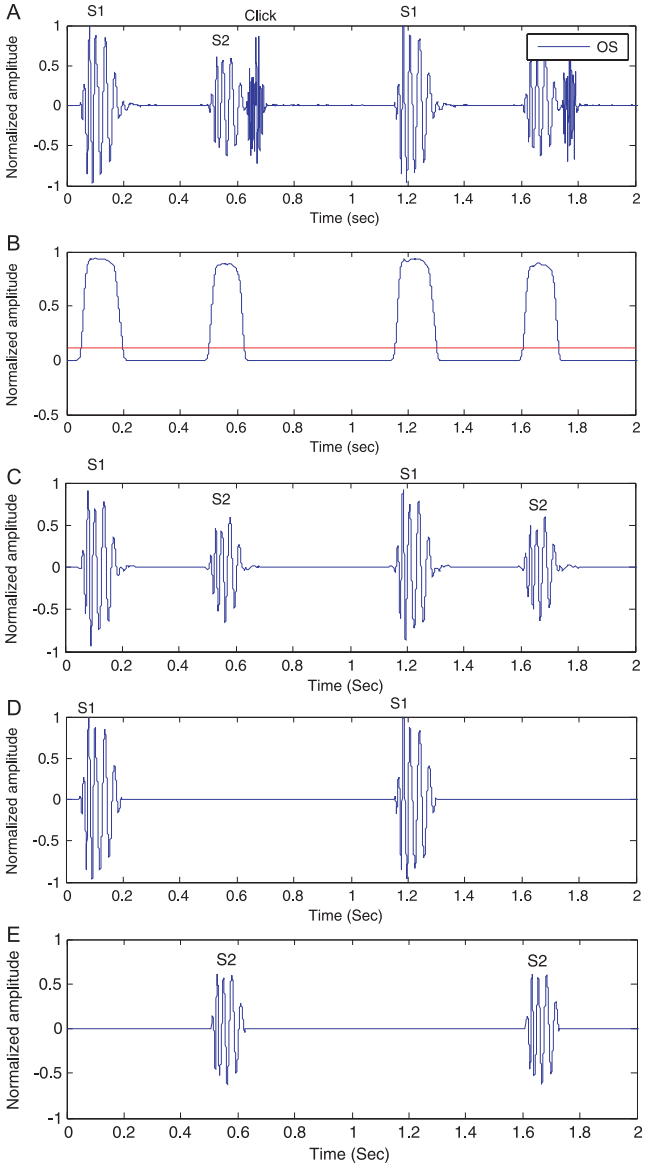

Figure 17. Insulation of heart sound: (a) PCG signal—OS (open snap); (b) energy envelope with a threshold of 90% of the maximum value; (c) heart sounds S1 and S2; (d) heart sound S1; (e) heart sound S2.

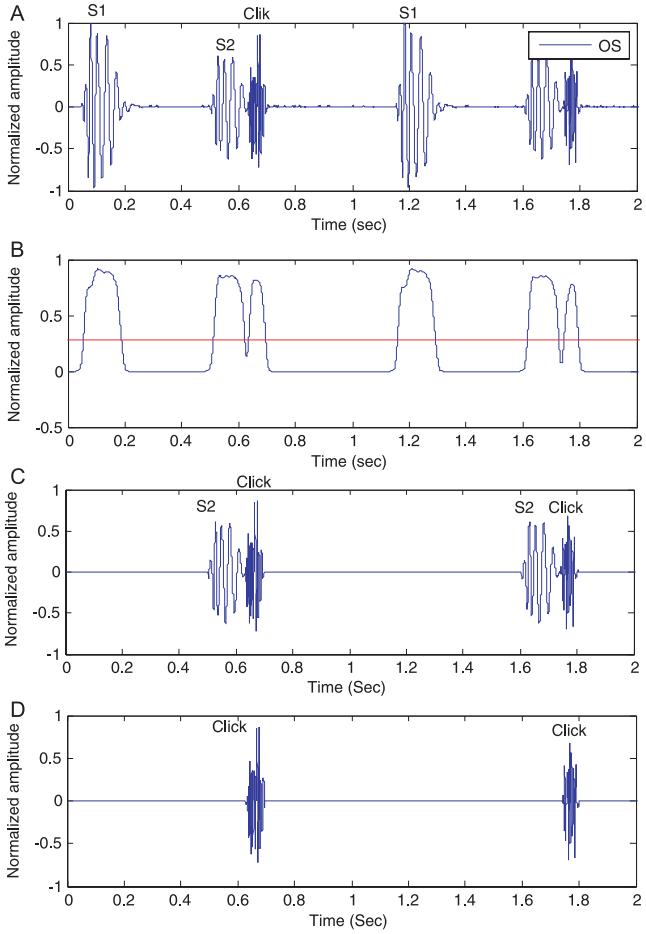

Figure 18. Insulation of heart sound: (a) PCG signal—OS (open snap); (b) energy envelope with a threshold of 80% of the maximum value; (c) heart sounds S2 and click; (d) heart click with a threshold of 80% of the maximum value.

and identification of different sounds. The Shannon energy envelope is used in this detection. The algorithm of segmentation was applied here for the separation of the S1 and S2 heart sounds of various PCG signals (using the first part of the proposed algorithm). This identification of heart sounds is based essentially on detection of different peaks of the envelope. This is done by manually applying a threshold set.

It is known beforehand that the duration of systole is shorter than that of the diastole. Based on this reality, the identification of sound S1 and S2 can be performed. The detection of the first and the second heart sound (S1, S2) can be done using the following conditions:

$$\begin{aligned} &\text{If } t(i+1)-t(i)<t(i+2)-t(i+1) \\ &\text{then } S1=P(i) \text{ and } S2=P(i+1) \end{aligned} \tag{13}$$

In fact, in this step the Shannon energy envelope (Figure 13(a)) can be a very effective parameter not only in identifying S1 and S2 peaks (Figure 13(b)), but also in the detection of the beginning and end of the each heart sound.

The choice of threshold is very important in order to obtain interesting results. The duration of the heart sounds or heart murmurs may change if the choice of threshold is not taken into account (Figure 14).

3.2. Detection of heart murmurs and clicks

The choice of threshold is also important for detection of the heart murmurs. Thus, for each heart murmur or click, one chooses a precise threshold. Separation of murmurs and clicks is done with the same procedure applied to separate the first and the second heart sounds (using the second part of the proposed algorithm).

After applying our algorithm on different PCG signals, the results are very satisfactory. This shows the power of the approaches used in the detection of S1 and S2 sounds and extraction of murmurs. However, this algorithm is limited by the very complex cases, where the sounds are completely immersed in the murmurs.

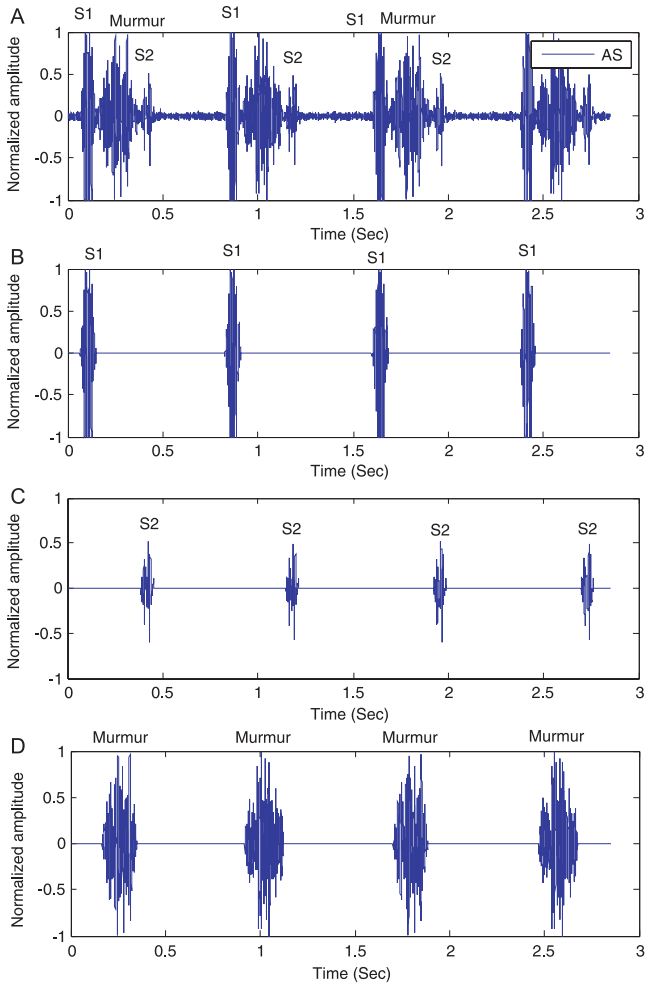

Figure 19. Insulation of heart murmurs: (a) PCG signal—AS (aortic stenosis); (b) heart sound S1 with a threshold of 80% of the maximum value; (c) heart sound S2 with a threshold of 80% of the maximum value; (d) systolic murmur envelope with a threshold of 80% of the maximum value.

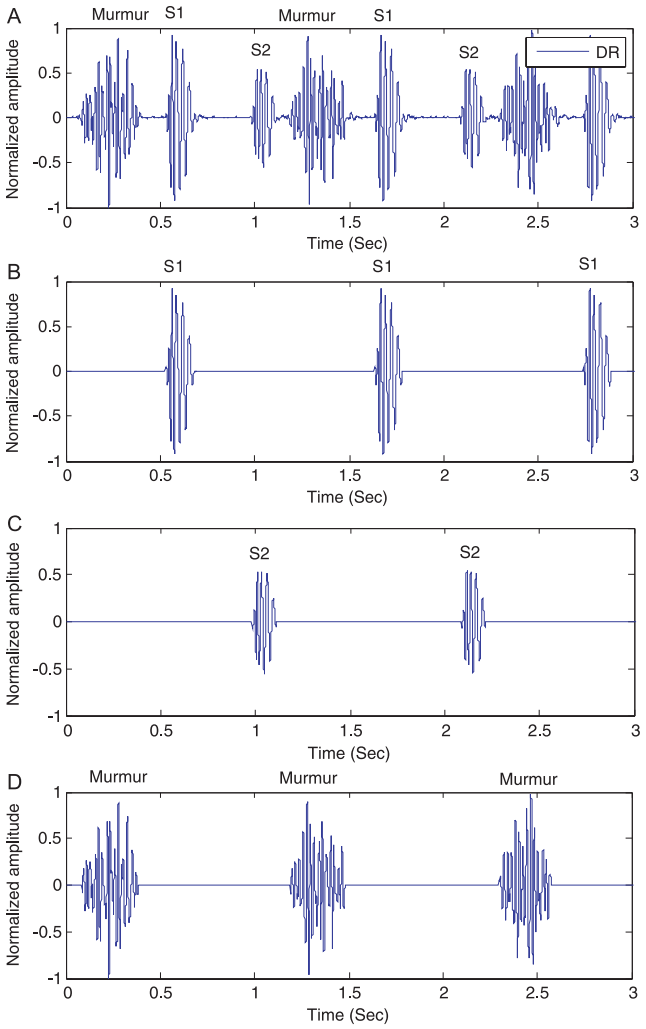

Figure 20. Insulation of heart murmurs. (a) PCG signal—DR (drum rumble); (b) heart sound S1 with a threshold of 90% of the maximum value; (c) heart sound S2 with a threshold of 90% of the maximum value; (d) diastolic murmur envelope with a threshold of 90% of the maximum value.

Figure 21 illustrates an example of this type of difficulty: if one does not have a location of the beginning and end moments of heart clicks, and even if we change the threshold of the energy envelope, we will not have satisfactory results.

To face this problem, we will use continuous wavelet transform (CWT) to provide a graphical extraction of the murmur. This has proven to be the best approach may well represent the time and frequency components of a signal (Figure 22).

4. Measurement of various parameters

After extraction of heart sounds and murmurs, several parameters can be obtained. The first parameter to determine is based on time–frequency representation by CWT. CWT (Figure 23) is applied to represent and analyse different PCG signal components (sounds, clicks or murmurs). This analysis can provide simultaneous information of the temporal extent (ΔT) and the frequency extent (ΔF) of both heart sounds and murmurs. It is possible to determine the temporal extent (ΔT) from the separation algorithm, when determining the beginning and end of the sounds.

Generally extended time and frequency sounds S1 and S2 can change from one signal to another but the graphical representation can not be very revealing. For this, the calculation of frequency and temporal rates (R_f,R_t) can greatly help to discover the likely differences between the normal and the pathological. In order to better quantify the differences existing between the sounds S1 and S2 of these signals we will consider the temporal and frequency rates shown as follows:

Let:

$$R_f = \left(\frac{\Delta F(S1) - \Delta F(S2)}{\Delta F(S2)} \right) \tag{14}$$

$$R_t = \left(\frac{\Delta T(S2) - \Delta T(S1)}{\Delta T(S1)} \right), \tag{15}$$

where ΔF is the frequency extent of the S1 or S2 sounds, and ΔT is the temporal extent of the S1 or S2 sounds.

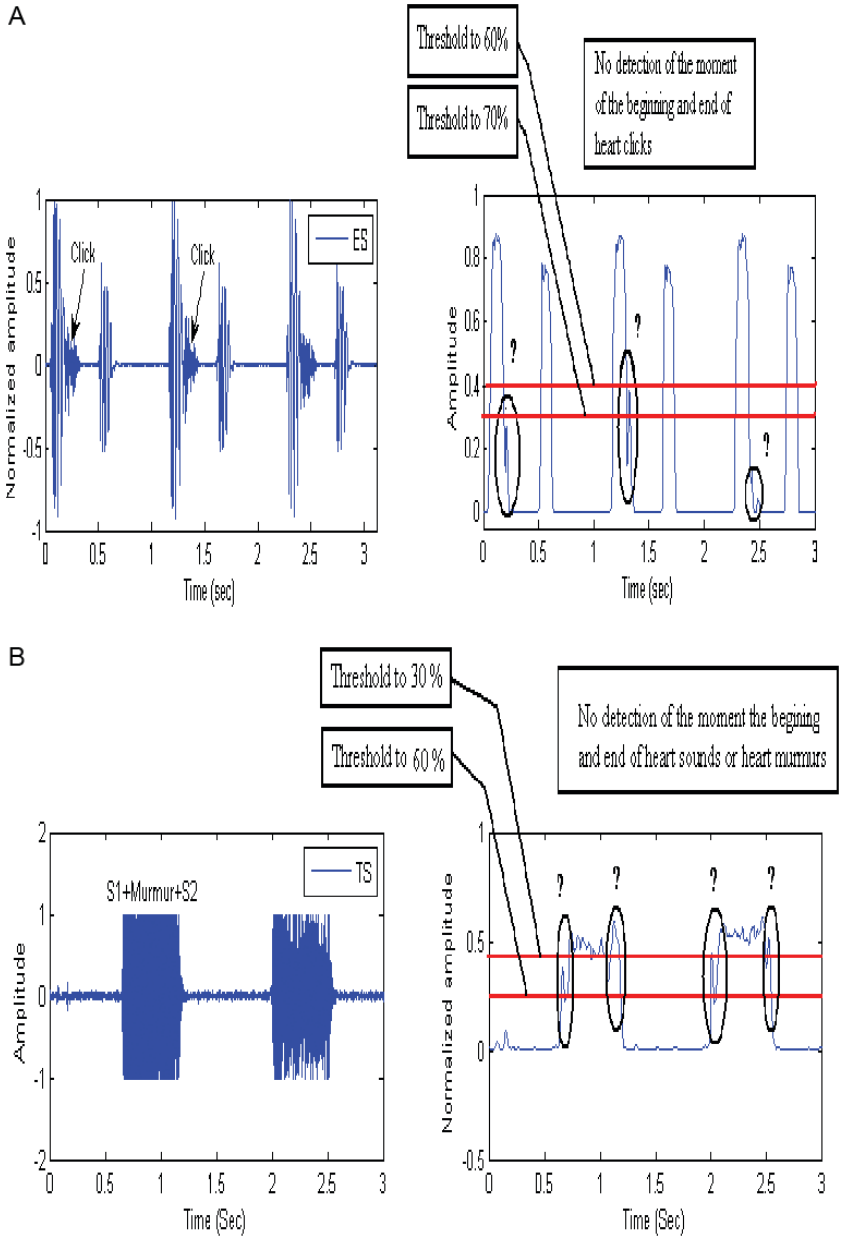

Figure 21. Limit of the method of separation on two examples: (a) early systolic (ES) PCG signal with clicks; (b) tricuspid stenosis (TS) PCG signal with murmurs.

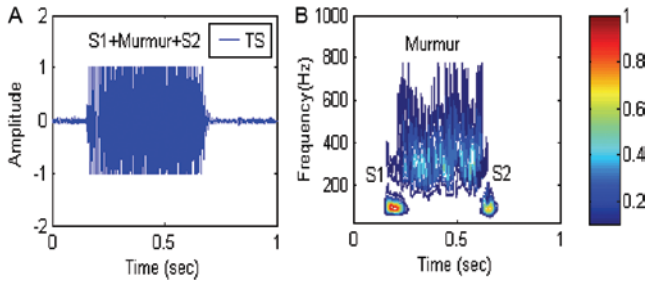

Figure 22. Time frequency analysis using continuous wavelet transform.

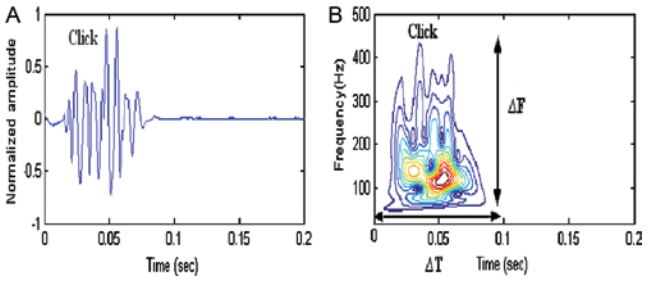

Figure 23. Analysis by continuous wavelet transform: (a) the temporal representation of a click; (b) CWT analysis.

However, more parameters can be obtained using DWT; in fact discrete wavelet transform performs better than CWT in term of separation of various PCG components.

In addition, the pathological analysis of signals by the use of discrete wavelet transform can reveal more or less important dissimilarities depending on the severity of disease or the existence

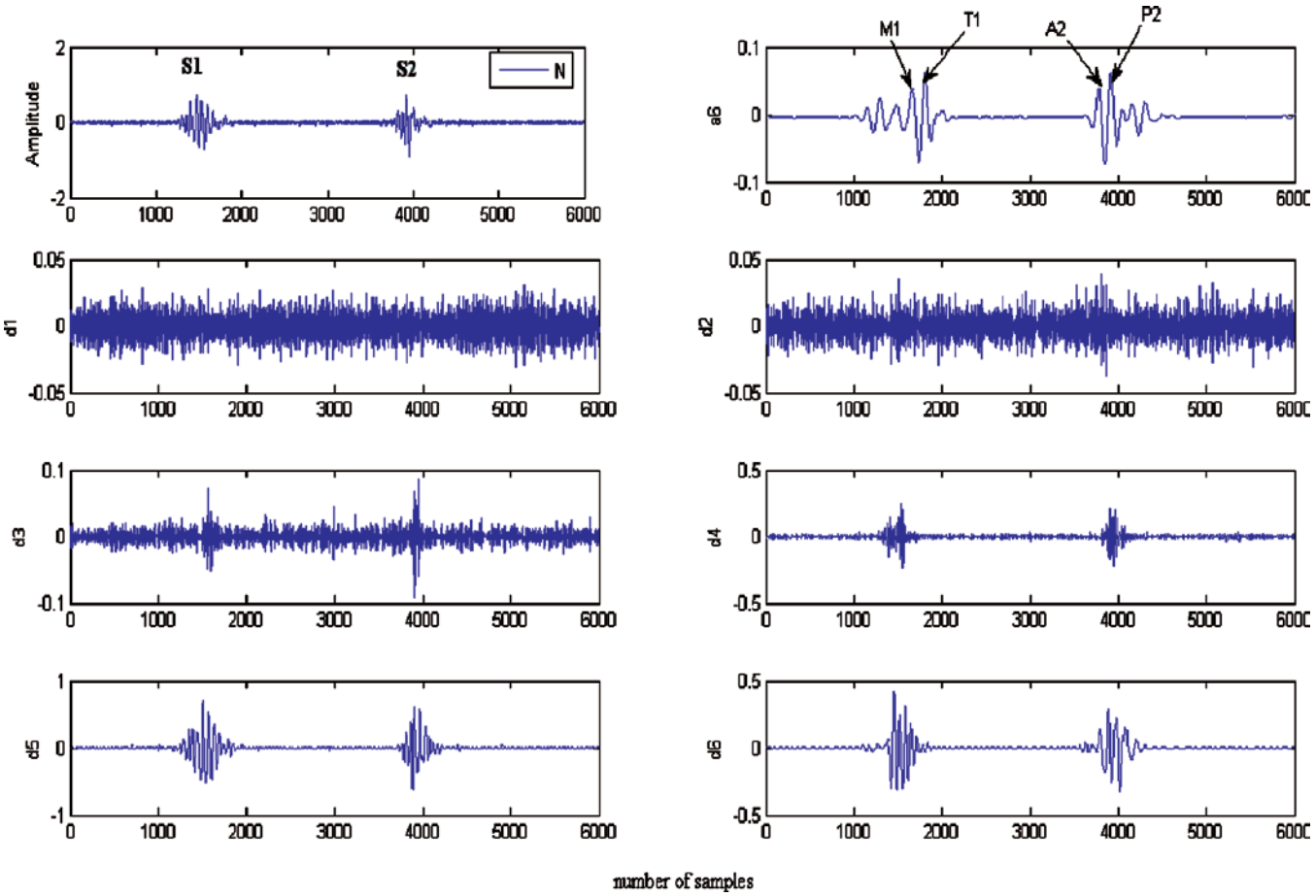

Figure 24. Analysis by discrete wavelet transform of a normal cycle of PCG.

of clicks or murmurs. To this end, we must establish a number of variables that can show easily and very visible all variations of PCGs signals relative to normal PCG signal.

In our work two parameters derived from the DWT analysis are used. The first parameter is the reconstruction error between the original signal and the reconstructed signal (a6) (Figure 24).

According to [25] this the reconstruction error parameter can be used successfully to estimate the degree of pathological severity. It is given by the following equation:

$$\xi_{ermoy} = \left(\frac{\sum_{1}^{N} |S_0(i) - S_r(i)|}{N} \right), \tag{16}$$

where S_0 = original signal; and S_r = reconstructed signal.

The reconstructed signal (a6) is obtained from the DWT. The second parameter that we can derive from the DWT analysis is the average variance of the details coefficients, denoted Md. Indeed, for all PCG signals used, we proceed to calculate the average variance of each detail level (d1 to d8). Then, a curve representing the variation of the average variance for the different levels of detail will be drawn. After that, a comparison between the obtained curves can be used to distinguish the difference between PCG signals and hence to ascertain the severity of disease. This first parameter can be calculated as follows:

$$M_d = \left(\frac{\sum_{1}^{N} d_{i,j}}{N} \right) \tag{17}$$

where $d_{i,j}$ is the ith coefficient of N retail level $\boldsymbol{j}$, and M_d is the average of the detail coefficients along the level $\boldsymbol{j}$.

5. Results and discussion

Three types of PCG signal are considered in our analysis:

- three PCG signals that have the same morphology as normal ones (Figure 25(a));
- three PCG signals with clicks (Figure 25(b));
- six PCG signals with murmurs (Figures 25(c) and 25(d)).

Table 1 gives more information about these signals. The first, second and third parameters mentioned in this section are calculated. The results are shown in Table 2.

Figures 26–29 show the result of the application of the CWT on the three signals categories, respectively.

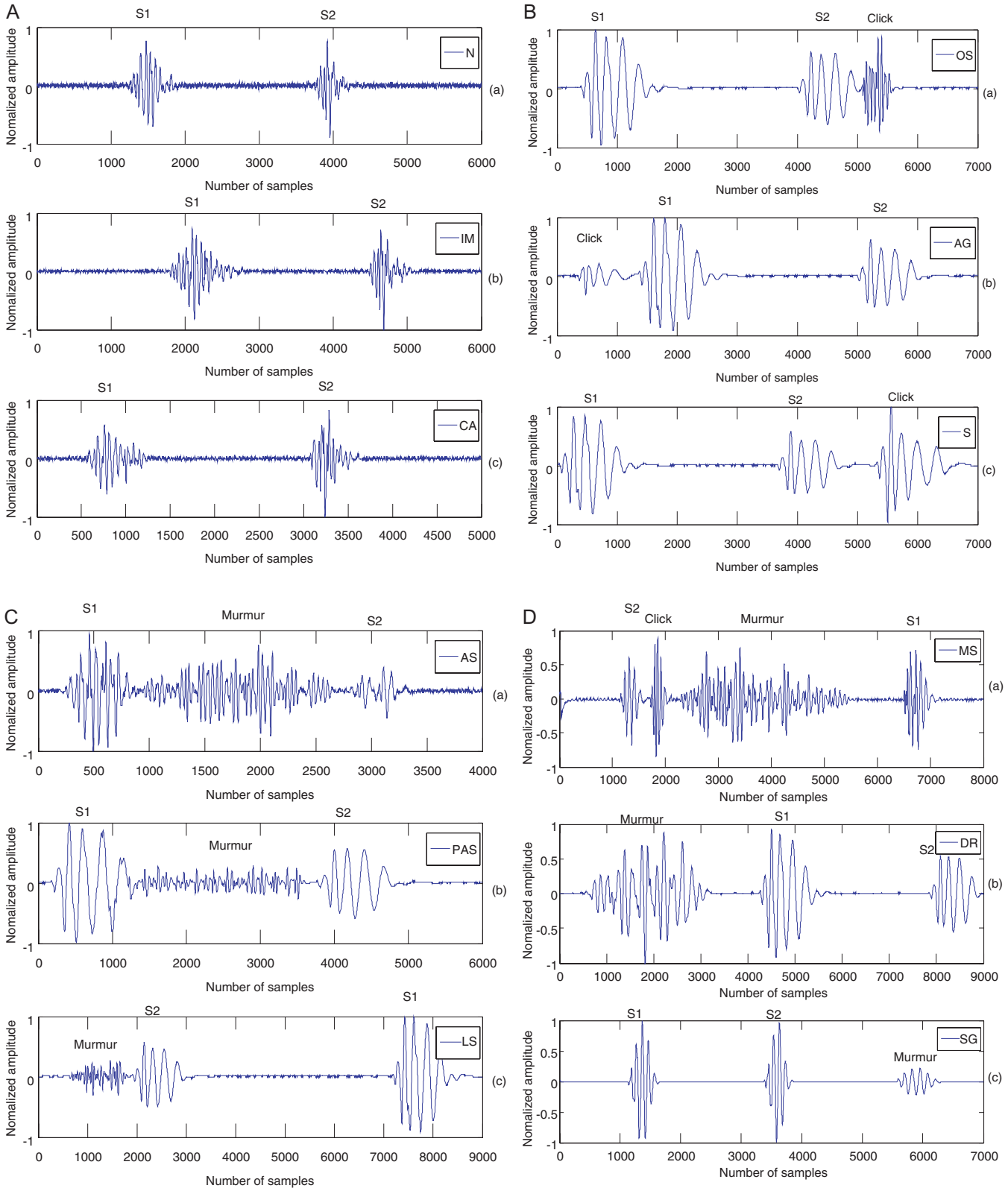

Figure 25. PCG signals.

The application of CWT on three PCG signals without murmur: normal, innocent murmur and coarctation of the aorta, is illustrated in Figure 26. The two heart sounds are clearly visible in this figure. The time interval between the first heart sound (S1) and second heard sound (S2), is 0.23, 0.21 and 0.2 seconds for normal PCG signal (N), innocent murmur (IM) and coarctation of the aorta (CA), respectively.

As is shown in Figure 26, the first heart sound S1 has a more significant temporal extent than the second heard sound (S2);

however the latter (S2) has higher frequency content than the first heart sound (S1 [27]). This is expected since the amount of blood present in the cardiac chambers is smaller [28].

The temporal extent (ΔT) and frequency range (ΔF) of the S1 and S2 hearts sounds provided by Table 2 can be measured easily from Figure 26. It can be seen according to R_t and R_f that the values of the rates concerning the IM case and the normal case approach much more than those of the case "CA". A time–frequency study of these three signals will confirm the results obtained here [25,26].

Figure 27 shows the results of application of CWT on PCG signals with clicks: opening snap (OS), atrial gallop (AG) and split diastolic (S). Measurements performed in this figure show that the first heart sound (S1) and the second heard sound (S2) of these pathological cases have a time and frequency extent different to signals without murmur.

This analysis explicitly shows that the first heard sound (S1) of the OS case and the second heart sound (S2) of AG and S cases have higher frequency content than that of the second heart sound (S2) of OS and first heart sound (S1) of AG and S. For the OS it is the significant variation of the frequency contents of the signal which is highlighted by the negative sign of the frequency rate R_f.

The first OS click has higher frequency content than that of the second and third click in AG and S, while their duration is larger than that of the OS click. This shows that the disease affects frequency extent more than duration. Consequently, we can conclude that OS click is more severe than the two AG and S clicks.

Table 1. The PCG signals used.

PCG signals	Abbreviation
PCG signals without murmurs	
Normal	N
Innocent murmur	IM
Coarctation of the aorta	CA
PCG signals with clicks	
Opening snap	OS
Arial gallop	AG
Split diastolic	S
PCG signals with murmurs	
Aortic stenosis	AS
Pulmonary stenosis	SP
Later systolic	LS
Mitral stenosis	MS
Drum rumble	DR
Summation gallop	SG

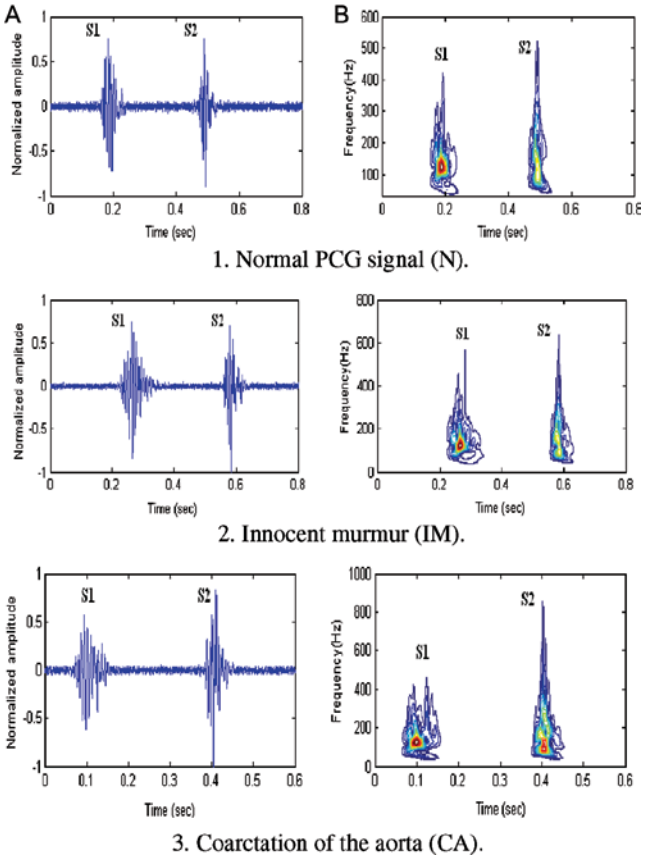

Figure 26. CWT analysis of PCG signals without murmurs that have the same morphology as the normal ones: N, IM and CA. (a) Temporal representation; (b) CWT analysis.

Table 2. Values of reporting frequency and time signals for the same PCG.

PCG signals	$\Delta T_{S1\ (sec)}$	$\Delta T_{S2(sec)}$	$\Delta T_{mur(sec)}$	$\Delta F_{S1(Hz)}$	$\Delta F_{S2(Hz)}$	$\Delta F_{mur(Hz)}$	R_f	R_t	Errmoy (10^{-3})
PCG signals without murmurs									
N	0.11	0.08		0.27	0.31		170	0.11	3.9365e–003
IM	0.11	0.07		0.36	0.17		187.3	0.11	4.02431e–003
CA	0.09	0.07		0.22	0.46		150	0.09	4.9163e–003
PCG signals with clicks									
OS	0.14	0.12	0.06	0.14	90.38	0.12	–0.04	0.14	11.6
AG	0.15	0.13	0.09	0.15	165.3	0.13	0.14	0.16	9
S	0.14	0.16	0.17	0.14	106.6	0.16	0.09	0.094	10.7
PCG signals with murmurs									
AS	0.08	0.05	0.19	200	180	360	–0.12	0.35	36
PAS	0.16	0.11	0.28	257.4	91.70	117	0.14	0.31	18
LS	0.17	0.14	0.13	62	85	174	0.37	0.17	7
MS	0.13	0.10	0.78	272	239	210	–0.12	0.23	29
DR	0.19	0.16	0.32	60	56	160	–0.35	–0.28	18
SG	0.08	0.07	0.09	155	160	64	0.03	0.12	6.5

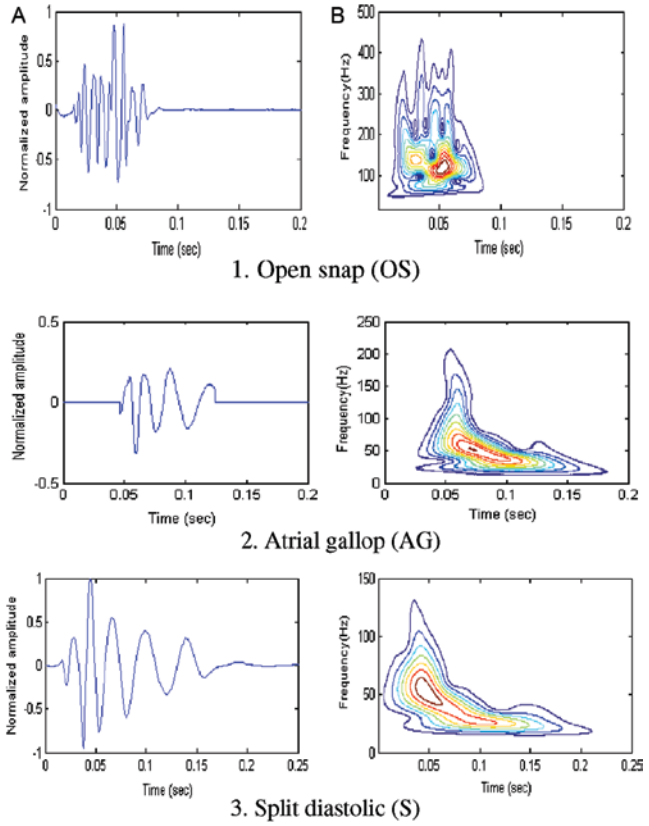

Figure 27. CWT analysis of PCG signals with clicks: OS, AG and S. (a) Temporal representation; (b) CWT analysis.

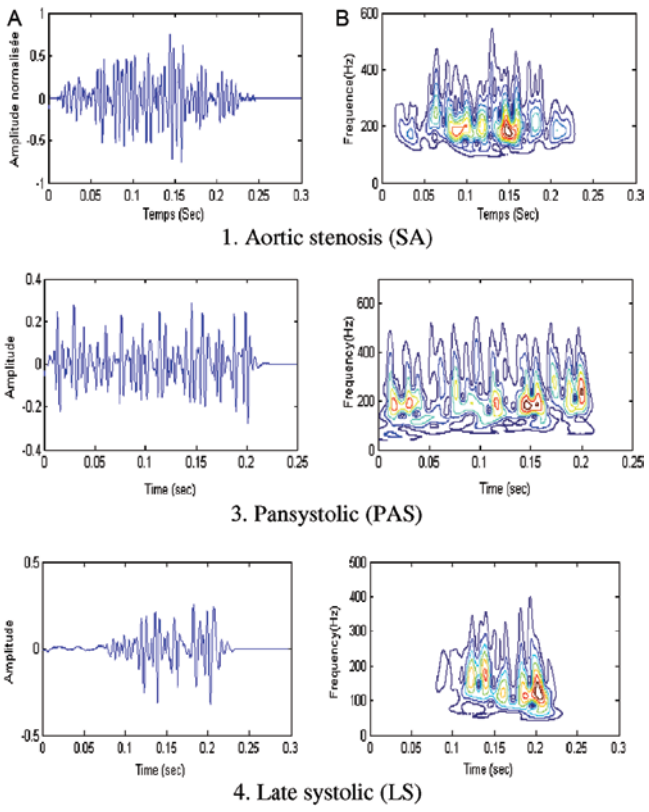

Figure 28. CWT analysis of PCG signals with systolic murmurs: AS, PAS and LS. (a) Temporal representation; (b) CWT analysis.

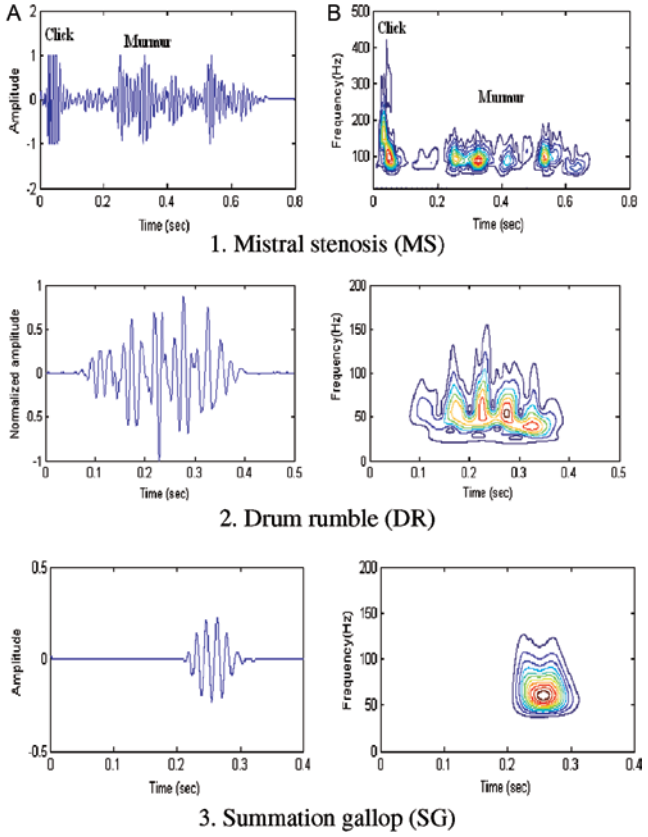

Figure 29. CWT analysis of PCG signals with diastolic murmurs: MS, DR and SG. (a) Temporal representation; (b) CWT analysis.

Figures 28 and 29 show that the frequency content of murmur is completely different to that of the hearts sounds and clicks. Moreover and according to Table 2, diastolic murmurs have more important frequency and temporal extents than the systolic ones. Further, for aortic stenosis (AS), mistral stenosis (MS) and drum rumble (DR), the significant variation of the frequency contents of the signals which is highlighted by the negative sign of the frequency rate R_f. Also for DR, it is the significant variation of the temporal contents of the signal which is highlighted by the negative sign of the temporal rate R_t. This could be possibly explained by the significant variation of the temporal delay (or split) between the two major components of the second cardiac sound S2, aortic (A2) and pulmonary (P2 [25]).

According to values provide in Table 2 and Figures 28 and 29 it can be seen that the time and frequency content of murmur is also important. The time and frequency content of the systolic murmur of the late systolic (LS) case is less important than other cases with a systolic murmur. The same is true for the diastolic murmur, summation gallop (SG). From the previous results, we can claim that the disease severity is related to frequency and temporal extent of murmur but to not the disease itself.

Using DWT analysis, the reconstruction error seems very useful parameter. Figure 30 represents the variation of the reconstruction error of PCG signals depending on the type and the growing importance of their murmurs. This confirms the validity of the choice of the reconstruction error as a parameter of classification.

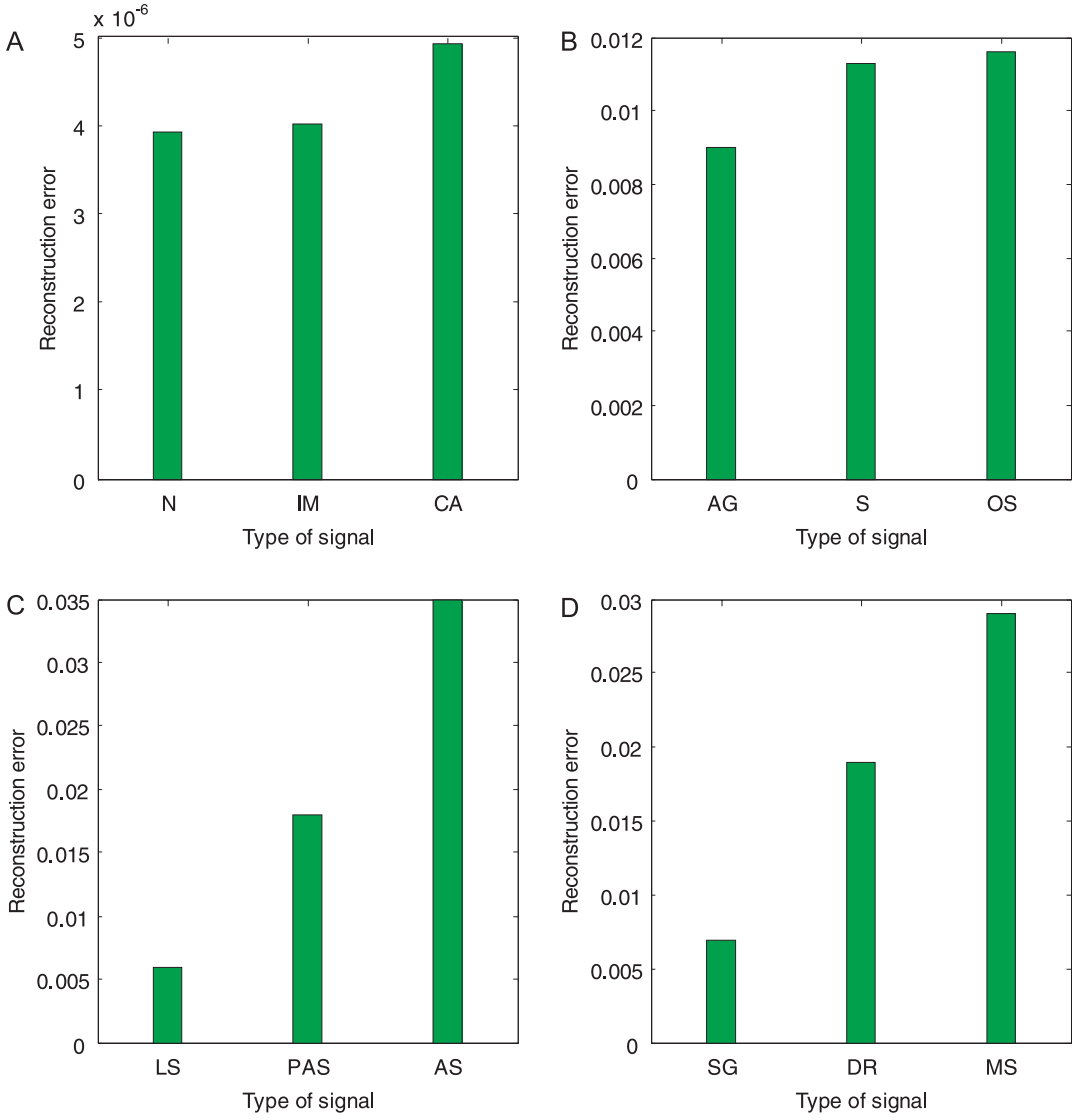

Figure 30. Variation of reconstruction errors.

The first remark to note is that the PCG signals of the first group, N, IM and CA, have the smaller error values.

Figure 30(a) shows that the reconstruction error of the normal case, N, is closer to the IM case, but it is different than that of the CA case which has a greater error. This means that IM is less severe than CA.

We can also notice that the second PCG signal category (Figure 30(b)), which represents signals with clicks, has a reconstruction error more significant than the first category. S and OS have greater errors than AG. These results confirm that this parameter is related to the increasing importance of the click. And they confirm that the AG case is less severe than S and OS cases.

The third PCG signal category (Figure 30(c)), which represents signals with murmurs, has a more significant reconstruction error than the first and second categories. AS and SP PCG signals have a reconstruction error greater than LS. Similarly for diastolic murmur signals, for MS and DR the reconstruction error is more significant than for SG. This is due to the fact that these PCG signal severities are more important than for MS and DR.

As mentioned previously, more parameters can be extracted from the DWT analysis. The Md parameters discussed in this section are illustrated in Figure 31(a). We can observe that the IM curve is closer to the normal one than the CA curve. Thus IM is less severe than the CA pathology. This result confirms the results obtained by CWT analysis.

Figure 31(b) represents the average variance variation curves for PCG signals with clicks. Figure 31(b) shows clearly that dissimilarities may exist between the three click types. OS and S click curves are much closer than the AG curve. At the seventh level of detail, the average variance values of these two clicks are 0.0056 and 0.0043, respectively. As a result, these two click types can be classified in the same severity degree group.

The Md parameter for the systolic breaths shows that dissimilarities exist between different breath types. The maximum average variance of AS is 0.0027. This value

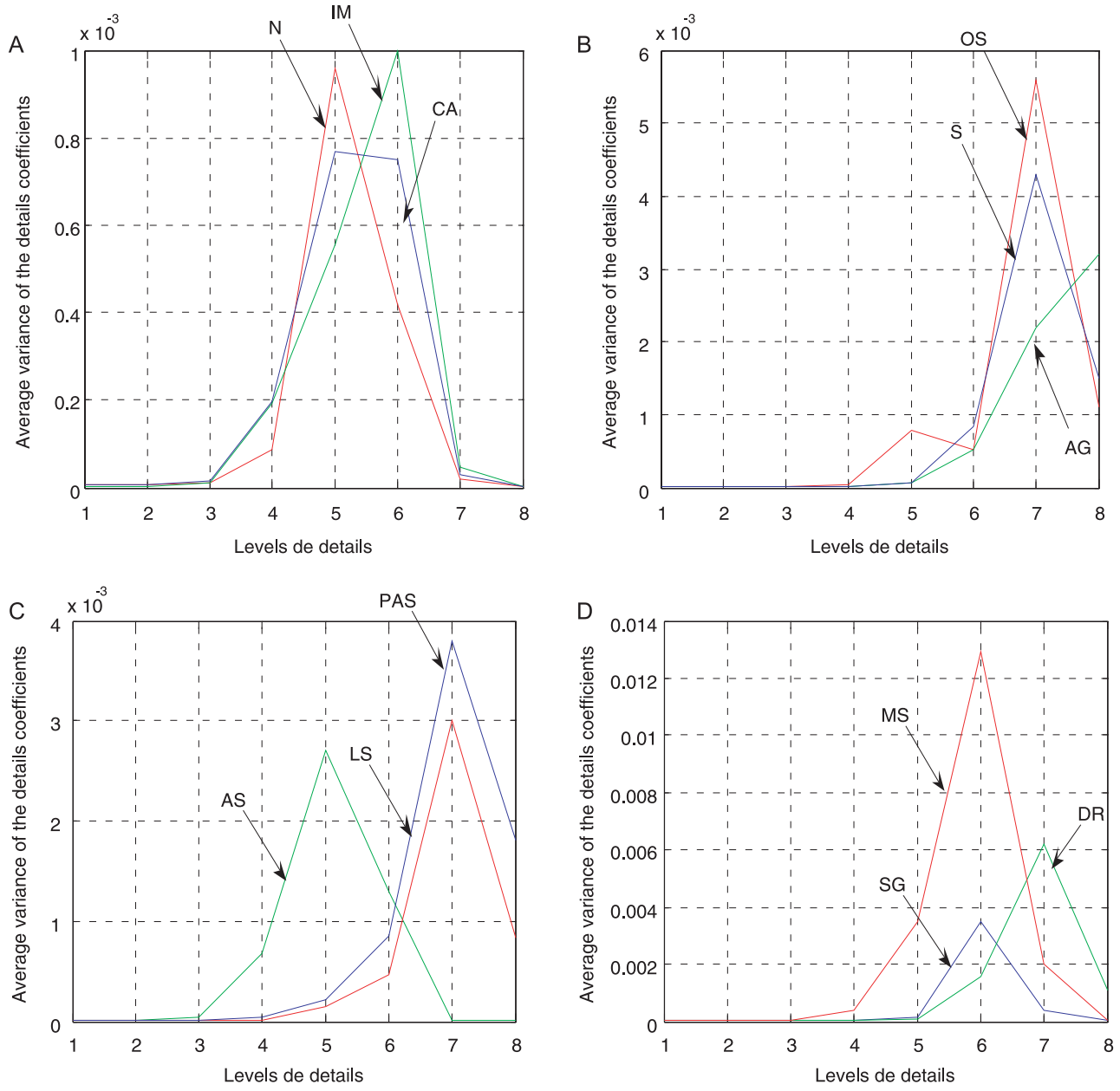

Figure 31. Average variance of detail coefficients for each decomposition level by applying discrete wavelet transform (DWT).

appears in the fifth level. The appearance of the maximum values at this lower level explains that AS is more energetic and thus is very severe. The maximum values of the LS and PAS case are 0.0029 and 0.0038, respectively, in the seventh level.

Figure 31(c) represents the Md curves of the MS, RD and SG diastolic murmurs. We can notice that diastolic murmurs have Md values greater than the systolic ones. In addition, the average variance values of the diastolic murmurs are proportional to temporal extent of the murmur. Consequently, we can conclude that the disease affects temporal extent more than frequency.

From this analysis we can conclude that the average of the detail coefficients Ad presents a relevant parameter to analyzeand classify the PCGs signals.

6. Conclusion

Analysis of phonocardiogram signals using wavelet transform is presented in this paper. At first, for diagnosis of heart sounds and heart murmurs, heart segmentation should be done. The proposed algorithm for segmenting of the phonocardiogram signal is based on wavelet denoising. With this segmentation, we can easily locate the S1 and S2 heart sounds, and extract the different systolic and diastolic murmurs. The obtained results are promised. In fact the good performances of our algorithm are related to the use of the energy envelope of Shannon and denoising by thresholding.

The choice of threshold is important so as to have interesting results; the duration measure of heart sounds or heart

murmurs may change if the choice of threshold is not taken into consideration.

After extraction of heart sounds and murmurs, several parameters can be obtained. The temporal and frequency rates seem to be very useful parameters for discrimination between various PCG signals. These parameters can help to discover the likely differences between normal and pathological PCG signals. The reconstruction error and the average variance of detail coefficients based on wavelet filtering (DWT), as measured and derived parameters, appear to be very important in the classification of PCG signals. Their variations are immediately linked to the growing importance of the murmur so but not to the severity of the disease being studied itself.

Declaration of interest: The authors state no conflict of interest.

References

[1] Beya, O., Bushra, J., Fauvet, E., and Laligant, O.L., 2009, *Application of EMD on cardiac signals (CNRIUT-Lille)*.

[2] Tilkian, A.G. and Conover, M.B., 1984, *Understanding Heart Sounds and Murmurs with an Introduction to Lung Sounds* (Philadelphia: Saunders).

[3] Djebbari, A. and Bereksi-Reguig, F., 2000, Short-time Fourier transform analysis of the phonocardiogram signal. *Proceedings of the IEEE conference*, **2**, 844–847.

[4] Domart, A. and Bourneuf, J., 1981, *New Medical Dictionary* (Paris: Librarie Larousse).

[5] Obaidat, M.S., 1993, Phonocardiogram signal analysis: techniques and performance comparison. *Journal of Medical Engineering & Technology*, **17**, 221–227.

[6] Tortora, G.J. and Grabowski, S.R., 2002, *Principles of Anatomy and Physiology.* F. Boudreault, M. Boyer and M.C. D'esorcy (Trans.), (Paris: De Boeck University), pp. 271–277.

[7] Mallat, S., 1989, Multiresolution approximations and wavelets orthonormal bases of L2(R). *Transactions of the American Mathematical Society*, **315**, 69–87.

[8] Tuteur, F.B., 1988, Wavelet transforms in signal detection. *IEEE ICASSP*, CH2561-9, 1435–1438.

[9] Grossmann, A., Holschneider, K.-M.R. and Morlet, J., 1987, Detection of abrupt changes in sound signal with the help of the wavelet transform. In: *Inverse Problems: an interdisciplinary study. Advances in Electronics and Electron Physics, Supplement 19* (New York: Academic), pp. 298–306.

[10] Mallat, S.G., 1989, A theory for multiresolution signal decomposition: the wavelet representation. *IEEE Transactions on Pattern Analysis and Machine Intelligence*, PAMI-11, 674–693.

[11] Soman, K.P. and Ramachandran, K.I.,2004, insight into wavelets from theory to practice 2nd edn. pp 15–22.

[12] Vikhe, P.S., Hamde, S.T. and Nehe, N.S., 28-29 December 2009, Wavelet transform based abnormality analysis of heart sound. *IEEE ICACCTT* (Trivandrum, Kerala, India), 28-29 December 2009, pp 368–369.

[13] Coifman, R. and Wickerhauser, M., 1995, Adapted waveform de-noising for medical signals and images. *IEEE Engineering in Medicine and BiomogyMagazine*, **14**(5), 578–586.

[14] Jacques P. deVos and Mike M. Blanckenberg., 2007.Automated Pediatric Cardiac Auscultation, *Journal of IEEE Transactions on Biomedical Engineering*, **54**(2), 244–252.

[15] Messer, S.R., Agzarian, J. and About, D., 2005, Optimal wavelet denoising for phonocardiograms. *Microelectronic Journal*, **32**, 931–941.

[16] Ranta, R., 2003, Wavelet denoising and segmentation for non-stationary signals: a reinterpretation of an iterative algorithm and application to phonoenterography. *Signal Processing*, **20**(2), 121–122.

[17] Donoho, D.L. and Johnstone, I.M., 1995, Adapting to unknown smoothness via wavelet shrinkage. *Journal of the American Statistical Association*, **90**(432), 1200–1224.

[18] Debbal, S.M. and Bereksi-Reguig, F., 2008, Pathological recognition of difference between phonocardiogram signals of similarly morphology using the wavelet transform. *Biomedical Soft Computing and Human Sciences*, **13**, 97–102.

[19] Akay, M., 1998, *Time Frequency and Wavelets in Biomedical Signal Processing* (New York: IEEE Press).

[20] Liang, H., Lukkarinen, S. and Hartimo, I., 1997, Heart sound segmentation algorithm based on heart sound envelogram. *Computers in Cardiology*, **24**, 105–108.

[21] Debbal, S.M. and Bereksi-Reguig, F., 2007, Features for heartbeat sound signal normal and pathological. *Journal of Recent Patents on Computer Science*, **1**(1), 1–8.

[22] Mgdob, H.M., Torry, J.N., Vincent, R. and Al-Naami, B., 2003, Application of Morlet transform wavelet in the detection of paradoxical splitting of the second heart sound. *IEEE Computers in Cardiology*, **30**, 323–326.

[23] Tovar-Corona, B. and Torry, JN., 1998, Time-frequency representation of systolic murmurs using wavelets. *IEEE Computers in Cardiology*, **25**, 601–604.

[24] Zin, Z.M., Salleh, S.H., Daliman, S. and Sulaiman, M.D., 2003, Analysis of heart sounds based on continuous wavelet transform.IEEE Conference on Research and Development, Putrajaya , Malaysia, 19–22.

[25] Debbal, S.M. and Bereksi-Reguig, F., 2005, Time-frequency analysis of the second cardiac sound in phonocardiogram. *Journal of Medical Physics*, **32**, 2911–2917.

[26] Debbal, S.M. and Bereksi-Reguig, F., 2004, The fast Fourier and the wavelet transforms analysis of the cardiac sounds. *Journal of Physical & Chemical News (PCN)*, **15**, 54–59.

[27] Debbal, S.M. and Bereksi-Reguig, F., 2004, The fast Fourier transform and continuous wavelet transforms analysis of the phonocardiogram signal. *Journal of Mechanics in Medicine and Biology (JMMB)*, **4**, 257–272.

[28] Ksembulingam and Prema Sembulingam, 2003, *Text Book of Essentials of Medical Physiology, 2nd edn,* New Delhi: Jaypee Brothers Medical Publishers(P)Ltd., pp 418–423.